J. Fluid Mech. (2013), *vol.* 718, *pp.* 371–397. © Cambridge University Press 2013
doi:10.1017/jfm.2012.617

Nonlinear long waves over a muddy beach

Erell-Isis Garnier[1], Zhenhua Huang[2] and Chiang C. Mei[3],†

[1]Department of Mechanical Engineering, Massachusetts Institute of Technology, 77 Massachusetts Avenue, Cambridge, MA 02139, USA

[2]School of Civil and Environmental Engineering, Nanyang Technological University, 50 Nanyang Avenue, Singapore 639798

[3]Department of Civil and Environmental Engineering, Massachusetts Institute of Technology, 77 Massachusetts Avenue, Cambridge, MA 02139, USA

(Received 16 May 2012; revised 26 November 2012; accepted 10 December 2012; first published online 8 February 2013)

We analyse theoretically the interaction between water waves and a thin layer of fluid mud on a sloping seabed. Under the assumption of long waves in shallow water, weakly nonlinear and dispersive effects in water are considered. The fluid mud is modelled as a thin layer of viscoelastic continuum. Using the constitutive coefficients of mud samples from two field sites, we examine the interaction of nonlinear waves and the mud motion. The effects of attenuation on harmonic evolution of surface waves are compared for two types of mud with distinct rheological properties. In general mud dissipation is found to damp out surface waves before they reach the shore, as is known in past observations. Similar to the Eulerian current in an oscillatory boundary layer in a Newtonian fluid, a mean displacement in mud is predicted which may lead to local rise of the sea bottom.

Key words: geophysical and geological flows, surface gravity waves, viscoelasticity

1. Introduction

There are many sea coasts in the world where the seabed is covered with fluid mud which is a mixture of water, fine and cohesive clay particles and sand. Dissipation in the mixture is considerably higher than in the pure sea water and causes very effective damping of waves arriving from the open sea. In turn the waves can induce changes of the muddy seabed and alter the coastal morphology in the long term.

For steady flows in muddy rivers numerous experiments have shown that the fluid mud can be approximated as a Bingham plastic material (Liu & Mei 1989; Wan 1994; Coussot 1997). However, for fluid mud in oscillatory flows rheological experiments are relatively scarce. Limited laboratory tests of natural mud by oscillatory rheometers have however indicated that viscoelastic properties are prevalent (Huang, Huhe & Zhang 1992; Jiang & Mehta 1995; Dalrymple, Nouri & Sabouri-Shargh 2008; Huang & Huhe 2009). In existing theoretical models different idealizations have been proposed mostly for wave/mud interaction over a horizontal seabed. Some authors have adopted the mathematically convenient Newtonian viscous model with vastly contrasting viscosities (Dalrymple & Liu 1978; Ng 2000; Liu & Chan 2007*a*). Others

† Email address for correspondence: ccmei@mit.edu

https://doi.org/10.1017/jfm.2012.617 Published online by Cambridge University Press

have proposed Bingham plastic models based only on rheometer tests of unidirectional flows (Mei & Liu 1987; Liu & Mei 1989). It is known that under waves fluid mud behaves more as a visco-elastic material. So far simple Kelvin–Voigt models with only two or three constant coefficients have been used (MacPherson 1980; Maa & Mehta 1988; Jiang & Mehta 1995; Ng & Zhang 2007; Liu & Chan 2007*a*,*b*).

Existing laboratory tests of natural fluid mud by using dynamic rheometers performing simple harmonic motions have however shown that the constitutive coefficients in the Kelvin–Voigt model depend strongly on frequency (Huang *et al.* 1992; Jiang & Mehta 1995; Huang & Huhe 2009). With increasing frequency, the shear modulus increases only mildly, but the viscosity μ decreases significantly and monotonically (Huang *et al.* 1992). Hence, the Kelvin–Voigt coefficients depend on the motion itself and are not just material properties. A remedy necessary for treating transient but non-sinusoidal problems is to use the generalized viscoelastic model relating the stress τ and strain $\mathscr{E}$, which reads, in one-dimensional motion,

$$\tau + \sum_{n=1}^{N} \alpha_n \frac{\partial^n \tau}{\partial t^n} = \beta_0 \mathscr{E} + \sum_{n=1}^{N} \beta_n \frac{\partial^n \mathscr{E}}{\partial t^n} \tag{1.1}$$

(see Malvern 1969). The coefficients α_n and β_n can be chosen to match the data of simple harmonic tests for the entire range of measured frequencies. In this way the constitutive coefficients depend only on material properties such as the mineral composition, particle size, concentration, etc and not on the frequency. For sinusoidal motions, the formally Kelvin–Voigt model with frequency-dependent coefficients is still meaningful. Using the measured data by Huang *et al.* (1992) (see also Huang & Huhe 2009), Mei *et al.* (2010) examined theoretically the effects of contrasting rheologies of fluid mud samples from two sites on the eastern coast of China on the evolution of narrow-banded waves in water of intermediate but constant depth. Asymptotic equations by Stokes-like expansions are derived for narrow-banded waves in water of finite depth. Damping rate and mud motion are examined at the first order of wave steepness, and long waves induced by radiation stresses at the second order. However, as is known for long waves over a rigid seabed, the Stokes expansion fails in very shallow water.

A prominent feature of a muddy beach is its ability to damp out essentially all incoming waves before they reach the shoreline. Wells (1978) first reported systematic field observations over a mud bank near the mouth of the Surinum River, Brazil, that incoming waves were all diminished to naught with no reflection or breaking (see also Wells & Coleman (1981)). This was confirmed by extensive measurements by Matthiew *et al.* (1995) on the Southern Coast of India, and Elgar & Raubenheimer (2008). An early attempt to explain this phenomenon was made by Miles (1983) who attributed the attenuation solely to the quadratic friction at the sea bottom without considering the mud rheology or wave nonlinearity.

The objective of this article is to develop a nonlinear theory suitable for long waves in a shallow seabed covered by fluid mud. Since generation of higher harmonics is expected in such a setting, the dependence of constitutive coefficients in frequencies is crucial for a realistic model of natural mud and is accounted for. Specifically we aim to examine the physical differences between two types of natural fluid mud with contrasting rheological properties. An asymptotic theory extending the Korteweg–de Vries approximation is derived in this study for analysing the combined effects of shoaling, nonlinearity, dispersion and dissipation. In addition we shall show that

https://doi.org/10.1017/jfm.2012.617 Published online by Cambridge University Press

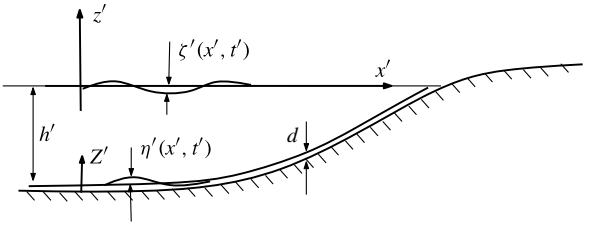


FIGURE 1. Water wave over a thin mud layer on a sloping seabed.

periodic waves can force steady mud displacement at the second order, analogous to acoustic streaming in an oscillating boundary layer in a Newtonian viscous fluid.

2. Assumptions

Referring to figure 1, we consider a shallow sea with a gently sloping bottom covered by a thin layer of fluid mud. The still water depth $h'(x')$ is assumed to be a slowly varying function of x' only, and the fluid mud is immiscible and of constant density ρ_M. Periodic waves propagate normally from the open sea toward a long and straight shore. In nature, the depth of the fluid mud layer changes with time and space, depending on the intensity and persistence of waves, degree of prior consolidation as well as erosion at the bottom and settling from the suspension above. In principle the depth as well as the density variation in the layer are unknown functions of the coupled motion between water and soil (Mehta 1996). For simplicity we assume the mean depth d of fluid mud to be constant. Predictions near the shore can of course be of qualitative validity at best.

Let A, k and h_0 be the reference wave amplitude, wavenumber and water depth, respectively. The wave dynamics is characterized by the following length ratios:

$$\epsilon = \frac{A}{h_0}, \quad \delta = \frac{d}{h_0} \quad \text{and} \quad \kappa = kh_0. \tag{2.1}$$

In this study, we assume

$$O(\epsilon) = O(\delta) = O(\kappa^2) \ll 1, \tag{2.2}$$

corresponding to the nonlinear dispersive waves of Boussinesq or Korteweg and de Vries. According to Green's law in the linearized theory of water waves over a sloping and rigid seabed, $\epsilon \sim A/h \propto h^{-5/4}$ and $\kappa = kh \propto h^{1/2}$ as h diminishes, hence nonlinearity can become so strong as to cause breaking near the shore. However, over a muddy bottom, dissipation in the mud layer also increases as the water depth decreases, and can become strong enough to counteract nonlinearity and reduce the tendency of breaking. To examine this possibility is an objective of this study.

As a preliminary, we first recall that under the stated conditions, the vertical displacement of the interface is much smaller than that of the sea surface (Liu & Mei 1989). For long waves in water, $\kappa = kh_0 \ll 1$ and $\omega = k\sqrt{gh_0}$. Mass conservation and the kinematic condition on the free surface require that

$$w' \sim (kh_0)u', \quad w' \sim \omega\zeta', \tag{2.3}$$

https://doi.org/10.1017/jfm.2012.617 Published online by Cambridge University Press

where u', w' are the vertical and horizontal velocities in water and ζ' the free-surface displacement in the vertical direction. In a mud layer of depth d, similar estimates give

$$W' \sim (kd)U', \quad W' \sim \omega\eta', \tag{2.4}$$

where U', W' are the mud velocities and η' the vertical displacement of the mud/water interface. Since for long waves in water over a thin mud layer, the horizontal pressure gradient in both water and mud is dominated by the free-surface slope $-g(\partial\zeta'/\partial x')$, balance of the horizontal momentum in both layers requires

$$\omega u' \sim gk\zeta' \sim \omega U' \tag{2.5}$$

which implies $u' \sim U'$. It follows that

$$\frac{\eta'}{\zeta'} \sim \frac{W'}{w'} \sim \frac{d}{h_0} \equiv \delta \ll 1. \tag{2.6}$$

Namely, the interface displacement is much smaller than that of the free surface.

3. Water layer

In comparison with fluid mud, sea water is much less viscous. Ignoring mixing, we assume the lutocline to be a sharp interface and the flow of water to be irrotational. The following normalization typical for long waves in shallow water is introduced

$$x = kx' \quad (z, h) = \frac{(z', h')}{h_0} \quad t = \omega t' \tag{3.1a}$$

$$p = \frac{p'}{\rho_W g A} \quad u = \frac{1}{(A/h_0)\sqrt{gh_0}}u' \quad w = \frac{kh_0}{(A/h_0)\sqrt{gh_0}}w' \tag{3.1b}$$

$$\zeta = \frac{\zeta'}{A} \quad \eta = \frac{\eta'}{(d/h_0)A} \quad \phi = \phi'\left[\frac{A}{kh_0}(gh_0)^{1/2}\right]^{-1} \tag{3.1c}$$

where (x', z') are the horizontal and vertical coordinates measured along and upward from the still water surface, respectively, p' is the water pressure, ϕ' is the velocity potential, ρ_W is the water density and $\omega = k\sqrt{gh_0}$ is the frequency of the long incident waves.

We first cite the exact field equations in dimensionless form. In water above the mud layer, the Laplace equation holds

$$\frac{\partial^2\phi}{\partial x^2} + \frac{\partial^2\phi}{\partial z^2} = 0, \quad -h + \epsilon\delta\eta < z < \epsilon\zeta. \tag{3.2}$$

The kinematic boundary condition on the free surface requires

$$\kappa^2\left(\frac{\partial\zeta}{\partial t} + \epsilon\phi_x\zeta_x\right) = \phi_z \quad \text{at } z = \epsilon\zeta. \tag{3.3}$$

The total pressure in water is given by the Bernoulli equation

$$-p = \phi_t + \frac{\epsilon}{2}\left[(\phi_x)^2 + \frac{1}{\kappa^2}(\phi_z)^2\right] + \frac{z}{\epsilon}. \tag{3.4}$$

Assuming zero surface pressure we have the following dynamic condition

$$\phi_t + \zeta + \frac{\epsilon}{2}\left[(\phi_x)^2 + \frac{1}{\kappa^2}(\phi_z)^2\right] = 0 \quad \text{at } z = \epsilon\zeta. \tag{3.5}$$

https://doi.org/10.1017/jfm.2012.617 Published online by Cambridge University Press

In addition to (2.2), we assume that the beach slope is so gentle that $\mathrm{d}h/\mathrm{d}x = O(\kappa^2)$ in dimensionless form. It is convenient to introduce a slow coordinate $X = \kappa^2 x$ so that $h = h(X)$.

Let

$$\bar{u} = \frac{1}{h + \epsilon(\zeta - \delta\eta)} \int_{-h+\epsilon\delta\eta}^{\epsilon\zeta} u \, \mathrm{d}z \tag{3.6}$$

be the depth-averaged horizontal velocity. From the exact depth-integrated law of mass conservation, we get by ignoring $\epsilon\delta(\eta\bar{u}) = O(\kappa^4)$,

$$\frac{\partial \zeta}{\partial t} - \delta \frac{\partial \eta}{\partial t} + \frac{\partial}{\partial x}\left[(h + \epsilon\zeta)\bar{u}\right] = O(\kappa^4). \tag{3.7}$$

By following Rayleigh's procedure of long-wave expansion (see e.g. Mei 1989),

$$\phi(x, z, t) = \phi^{(0)} + (z + h)\phi^{(1)} + \frac{(z+h)^3}{2}\phi^{(2)} + \cdots \tag{3.8}$$

where $\phi^{(n)}$ are functions of x, X, t only, and by applying the pressure-free condition on the free surface, we get the conservation equation for the depth-averaged horizontal momentum,

$$\frac{\partial \bar{u}}{\partial t} + \epsilon\bar{u}\frac{\partial \bar{u}}{\partial x} + \frac{\partial \zeta}{\partial x} - \frac{\kappa^2}{3}h^2 \frac{\partial^3 \bar{u}}{\partial x^2 \partial t} = O(\kappa^4). \tag{3.9}$$

Equations (3.7) and (3.9) are of the Boussinesq form, now modified for the soft bottom.

For later matching of normal stress with the mud layer, we need the dynamic water pressure on the interface. The total pressure on the interface can be shown to be

$$p = \frac{h(X)}{\epsilon} - \phi_t^{(0)} - \delta\eta - \frac{\epsilon^2}{2}(\phi_x)^2 + O(\epsilon\kappa^2) = \frac{h(X)}{\epsilon} + \zeta - \delta\eta + O(\epsilon\kappa^2) \quad \text{at } z = -h. \tag{3.10}$$

Thus, the dynamic water pressure on the interface is approximately

$$p_d = \zeta - \delta\eta + O(\epsilon\kappa^2) \quad \text{at } z = -h(X). \tag{3.11}$$

4. Fluid mud

4.1. *Viscoelastic properties of fluid mud*

In a few existing experiments it is known that fluid mud in oscillatory flows is decidedly viscoelastic rather than Bingham plastic. In past theories the linear model of Kelvin–Voigt of constant constitutive coefficients have been used:

$$\tau'_{ij} = G'\left(\frac{\partial \mathscr{U}'_i}{\partial x'_j} + \frac{\partial \mathscr{U}'_j}{\partial x'_i}\right) + \mu'\left(\frac{\partial U'_i}{\partial x'_j} + \frac{\partial U'_j}{\partial x'_i}\right), \tag{4.1}$$

where $\mathscr{U}'_i$ $(i = 1, 2, 3)$are the mud displacements and $U'_i = \partial \mathscr{U}'_i/\partial t'$ the corresponding velocity components. Rheological data from vibratory tests of field samples show that both G' and μ' depend not only on the mineral composition but also on the frequency ω of oscillation (Huang *et al.* 1992; Jiang & Mehta 1995; Dalrymple *et al.* 2008; Huang & Huhe 2009). For simple harmonic motion one can

https://doi.org/10.1017/jfm.2012.617 Published online by Cambridge University Press

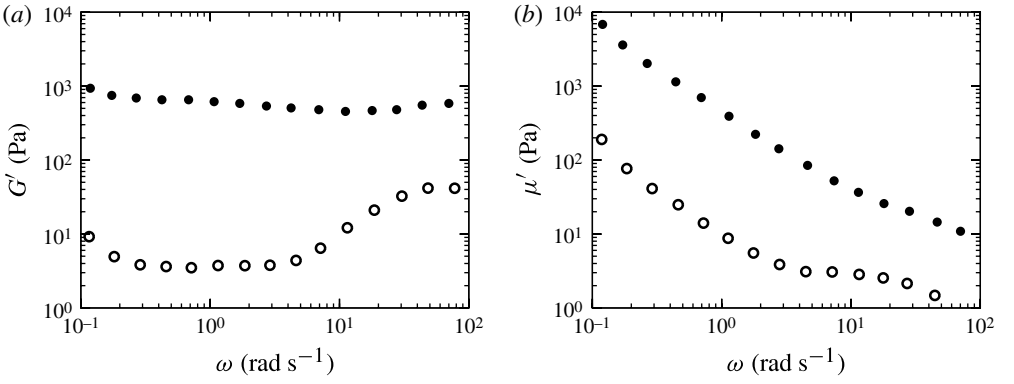


FIGURE 2. Shear modulus and viscosity of fluid mud from Hangzhou Bay (open circles) and Lianyun Harbor (solid circles). The mixture density is chosen to be the same for both Hangzhou Bay mud and Lianyun Harbor mud: $\rho_M = 1590\ \mathrm{kg\ m^{-3}}$. (Extracted from Huang *et al.* (1992).)

write $U_i' = \mathrm{Re}\{\widetilde{U}_i' \mathrm{e}^{-\mathrm{i}\omega t'}\}$, $\mathscr{U}_i' = \mathrm{Re}\{\widetilde{\mathscr{U}}_i' \mathrm{e}^{-\mathrm{i}\omega t}\}$ so that

$$\widetilde{\tau}_{ij}' = \left(\mu' + \mathrm{i}\frac{G'}{\omega}\right)\left(\frac{\partial \widetilde{U}_i'}{\partial x_j'} + \frac{\partial \widetilde{U}_j'}{\partial x_i'}\right). \tag{4.2}$$

A complex viscosity can be defined by

$$\mu_c' = \mu' + \mathrm{i}\frac{G'}{\omega} \equiv |\mu'|\mathrm{e}^{\mathrm{i}\theta} \tag{4.3}$$

which is a function of ω for a given mud, a property that will be accounted for in this study. Unlike the case of steady flows, so far there is no systematic experimental evidence that (4.2) needs nonlinear correction. In any case the linear rheological law is used only for the first-order motion in our second-order analysis later.

In this paper use will be made of the viscometric data of sea-bed samples from Hangzhou Bay, Zhejiang Province and from Lianyun Harbor, Jiangshu Province, China, measured in an oscillatory rheometer (RMS-605) for frequencies within the range of $0.1 < \omega < 100\ \mathrm{rad\ s^{-1}}$ and for a wide range of particle concentrations by controlled dilution (Huang *et al.* 1992; Huang & Huhe 2009). The Hangzhou Bay mud has relatively coarse grains with $D_{50} = 90\ \mu\mathrm{m}$ and grain density $\rho_s = 2704\ \mathrm{kg\ m^{-3}}$; for volume concentration of particles $\phi = 0.077$–0.340, the mixture density is $\rho_M = 1145$–$1590\ \mathrm{kg\ m^{-3}}$, where ϕ is the volume concentration defined by $\phi = (\rho_M - \rho)/(\rho_s - \rho)$ and ρ is the density of salt water. The Lianyun Harbor mud has very fine grains with $D_{37} = 5\ \mu\mathrm{m}, D_{85} = 50\ \mu\mathrm{m}$ and grain density $\rho_s = 2750\ \mathrm{kg\ m^{-3}}$; for a particle concentration $\phi = 0.049$–0.331, the mixture density is $\rho_M = 1100$–$1590\ \mathrm{kg\ m^{-3}}$. Figure 2 shows the shear modulus $G'(\omega)$ and viscosity $\mu'(\omega)$ for Hangzhou Bay mud and for Lianyun Harbor mud with the same $\rho_M = 1590\ \mathrm{kg\ m^{-3}}$.

Figure 2 also indicates that as ω becomes small, G' tends to a finite limit, implying the dominance of elasticity, characteristic of a Kelvin–Voigt material. For convenience the magnitude and phase of $\mu_c'(\omega)$ are also plotted in figure 3. Note that the Hangzhou Bay mud is less viscous and more Newtonian. On the other hand, the phase of

https://doi.org/10.1017/jfm.2012.617 Published online by Cambridge University Press

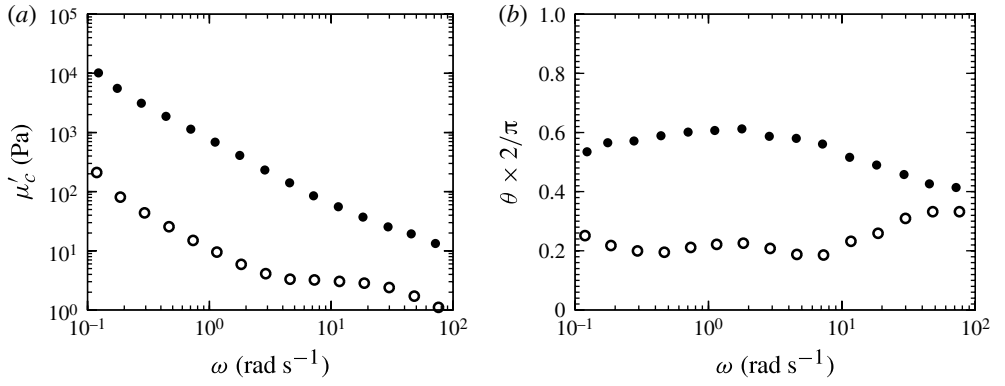


FIGURE 3. Modulus and phase of the complex viscosity of fluid mud from Hangzhou Bay (open circles) and Lianyun Harbor (solid circles). The mixture density is chosen to be the same for both Hangzhou Bay mud and Lianyun Harbor mud: $\rho_M = 1590\ \mathrm{kg\ m^{-3}}$. (Extracted from Huang *et al.* (1992).)

the mud from Lianyun Harbor is more close to $\pi/2$, implying high elasticity. The difference is the consequence of different particles size and mineral compositions.

4.2. *Approximate field equations for mud motion*

In the fluid mud it is convenient to employ a new vertical coordinate measured upward from the rigid bottom as shown in figure 1,

$$Z' = z' + h'(x') + d \tag{4.4}$$

so that the mud layer is in $0 < Z' < d$ and

$$\frac{\partial}{\partial z'} = \frac{\partial}{\partial Z'}, \quad \frac{\partial}{\partial x'} \to \frac{\partial}{\partial x'} + \frac{\mathrm{d}h'}{\mathrm{d}x'}\frac{\partial}{\partial Z'}. \tag{4.5}$$

Let us introduce the following normalization

$$x = kx' \quad Z = \frac{Z'}{d} \quad t = \omega t' \tag{4.6a}$$

$$P = \frac{P'}{\rho_W g A} \quad U = \frac{1}{\dfrac{A}{h_0}\sqrt{gh_0}}U' \quad W = \frac{1}{\dfrac{A}{h_0}kd\sqrt{gh_0}}W' \tag{4.6b}$$

$$\tau_{xx} = \frac{\tau'_{xx}}{\mu_s k\dfrac{A}{h_0}\sqrt{gh_0}}, \quad \tau_{xz} = \frac{\tau'_{xz}}{\dfrac{\mu_s}{d}\dfrac{A}{h_0}\sqrt{gh_0}}, \quad \tau_{zz} = \frac{\tau'_{zz}}{\mu_s k\dfrac{A}{h_0}\sqrt{gh_0}}, \quad \eta = \frac{\eta'}{\dfrac{d}{h_0}A} \tag{4.6c}$$

where uppercase letters U, W, P denote the velocities and pressure in the fluid mud, and μ_s the (real) characteristic scale of the complex viscosity.

In dimensionless form, the equation of mass conservation reads

$$\left(\frac{\partial}{\partial x} + \frac{\kappa^2}{\delta}\frac{\mathrm{d}h}{\mathrm{d}X}\frac{\partial}{\partial Z}\right)U + \frac{\partial W}{\partial Z} = 0, \quad 0 < Z < 1 + \epsilon\eta, \tag{4.7}$$

https://doi.org/10.1017/jfm.2012.617 Published online by Cambridge University Press

and the exact equation of horizontal momentum is

$$\frac{\partial U}{\partial t}+\epsilon\left[U\left(\frac{\partial}{\partial x}+\frac{\kappa^2}{\delta}\frac{\mathrm{d}h}{\mathrm{d}X}\frac{\partial}{\partial Z}\right)U+W\frac{\partial U}{\partial Z}\right]$$
$$=-\gamma\left(\frac{\partial}{\partial x}+\frac{\kappa^2}{\delta}\frac{\mathrm{d}h}{\mathrm{d}X}\frac{\partial}{\partial Z}\right)P_d+\frac{1}{R}\left[\frac{\partial\tau_{xz}}{\partial Z}+\kappa^2\delta^2\left(\frac{\partial\tau_{xx}}{\partial x}+\frac{\kappa^2}{\delta}\frac{\mathrm{d}h}{\mathrm{d}X}\frac{\partial\tau_{xx}}{\partial Z}\right)\right], \quad (4.8)$$

where P_d is the hydrodynamic pressure in the mud layer, $\gamma=\rho_W/\rho_M$ is the ratio of densities and R is the Reynolds number defined by

$$R=\frac{\rho_M\omega d^2}{\mu_s}. \quad (4.9)$$

Formally, $\sqrt{R}$ is the ratio of mud depth to the Stokes boundary layer thickness.

For later examination of the time-averaged response in the mud layer, we keep terms of $O(1)$ and $O(\kappa^2,\epsilon,\delta)$ in the horizontal momentum equation,

$$\frac{\partial U}{\partial t}-\frac{1}{R}\frac{\partial\tau_{xz}}{\partial Z}=-\gamma\frac{\partial P_d}{\partial x}-\frac{\kappa^2}{\delta}\gamma\frac{\mathrm{d}h}{\mathrm{d}X}\frac{\partial P_d}{\partial Z}-\epsilon\left(U\frac{\partial U}{\partial x}+\frac{\kappa^2}{\delta}\frac{\mathrm{d}h}{\mathrm{d}X}U\frac{\partial U}{\partial Z}+W\frac{\partial U}{\partial Z}\right)+O(\epsilon^2). \quad (4.10)$$

In dimensionless variables, the vertical momentum equation reads

$$\frac{\partial W}{\partial t}+\epsilon\left[U\left(\frac{\partial}{\partial x}+\frac{\kappa^2}{\delta}\frac{\mathrm{d}h}{\mathrm{d}X}\frac{\partial}{\partial Z}\right)W+W\frac{\partial W}{\partial Z}\right]$$
$$=-\frac{\gamma}{\kappa\delta}\frac{\partial P_d}{\partial Z}+\frac{1}{R}\left[\frac{\partial\tau_{zz}}{\partial Z}+\left(\frac{\partial}{\partial x}+\frac{\kappa^2}{\delta}\frac{\mathrm{d}h}{\mathrm{d}X}\frac{\partial}{\partial Z}\right)\tau_{xz}\right]. \quad (4.11)$$

Hence

$$\frac{\partial P_d}{\partial Z}=O(\delta^2)=O(\epsilon^2), \quad 0<Z<1+\epsilon\eta, \quad (4.12)$$

as is expected in a thin layer. Consequently (4.10) can be further simplified to

$$\frac{\partial U}{\partial t}-\frac{1}{R}\frac{\partial\tau_{xz}}{\partial Z}=-\gamma\frac{\partial P_d}{\partial x}-\epsilon\left(U\frac{\partial U}{\partial x}+\frac{\kappa^2}{\delta}\frac{\mathrm{d}h}{\mathrm{d}X}U\frac{\partial U}{\partial Z}+W\frac{\partial U}{\partial Z}\right)+O(\epsilon^2). \quad (4.13)$$

4.3. *Boundary conditions*

At the bottom, we impose the no-slip condition,

$$U=W=0 \quad \text{at } Z=0. \quad (4.14)$$

On the interface defined by $Z-(1+\epsilon\eta)=0$, the exact kinematic constraint of tangential motion reads

$$-\frac{\partial\eta}{\partial t}-\epsilon U\frac{\partial\eta}{\partial x}+\frac{\kappa^2}{\delta}U\frac{\mathrm{d}h}{\mathrm{d}X}+W=0 \quad \text{at } Z=1+\epsilon\eta. \quad (4.15)$$

In physical variables, continuity of vertical and horizontal stresses on the mud/water interface requires, exactly,

$$\tau'_{xz}n_x+(-P'_d+\tau'_{zz})n_z=-p'_dn_z \quad \text{at } Z'=d+\eta', \quad (4.16a)$$
$$(-P'_d+\tau'_{xx})n_x+\tau'_{xz}n_z=-p'_dn_x \quad \text{at } Z'=d+\eta', \quad (4.16b)$$

https://doi.org/10.1017/jfm.2012.617 Published online by Cambridge University Press

where P'_d and p'_d are, respectively, the dynamic pressure in mud and water. The dimensionless stress conditions are

$$\frac{\delta\kappa}{\gamma R}\tau_{xz}n_x + \left(-P_d + \frac{\delta^2\kappa^2}{\gamma R}\tau_{zz}\right)n_z = -p_d n_z \quad \text{at } Z = 1+\epsilon\eta, \tag{4.17a}$$

$$\left(-P_d + \frac{\delta\kappa}{\gamma R}\tau_{xx}\right)n_x + \frac{\delta\kappa}{\gamma R}\tau_{xz}n_z = -p_d n_x \quad \text{at } Z = 1+\epsilon\eta. \tag{4.17b}$$

For a gently sloping interface, the components of the unit normal can be approximated by

$$n_x = \frac{\kappa^3\dfrac{\mathrm{d}h}{\mathrm{d}X} + \epsilon\delta\kappa\dfrac{\partial\eta}{\partial x}}{\sqrt{1+\left(\kappa^3\dfrac{\mathrm{d}h}{\mathrm{d}X} + \epsilon\delta\kappa\dfrac{\partial\eta}{\partial x}\right)^2}} = \kappa^3\frac{\mathrm{d}h}{\mathrm{d}X} + O(\kappa^6), \tag{4.18a}$$

$$n_z = \frac{1}{\sqrt{1+\left(\kappa^3\dfrac{\mathrm{d}h}{\mathrm{d}X} + \epsilon\delta\kappa\dfrac{\partial\eta}{\partial x}\right)^2}} = 1 + O(\kappa^6). \tag{4.18b}$$

It follows from (4.16) that

$$P_d - p_d = O(\delta\kappa^4) \quad \text{at } Z = 1+\epsilon\eta \tag{4.19}$$

and

$$\tau_{xz} = \gamma R(P_d - p_d)\frac{\kappa^2}{\delta}\frac{\mathrm{d}h}{\mathrm{d}X}\left(1+O(\kappa^4)\right) = O(\kappa^4) \quad \text{at } Z = 1+\epsilon\eta. \tag{4.20}$$

Using (3.11) we get

$$P_d = \zeta - \delta\eta + O(\epsilon\kappa^2), \quad 0 < Z \leqslant 1+\epsilon\eta \tag{4.21}$$

which can be used to rewrite the horizontal momentum equation (4.13) of mud as

$$\frac{\partial U}{\partial t} - \frac{1}{R}\frac{\partial\tau_{xz}}{\partial Z} = -\gamma\left(\frac{\partial\zeta}{\partial x} - \delta\frac{\partial\eta}{\partial x}\right) - \epsilon\left(U\frac{\partial U}{\partial x} + \frac{\kappa^2}{\delta}\frac{\mathrm{d}h}{\mathrm{d}X}U\frac{\partial U}{\partial Z} + W\frac{\partial U}{\partial Z}\right) + O(\kappa^4), \quad 0 < Z < 1+\epsilon\eta. \tag{4.22}$$

Together with the requirements of vanishing shear (4.20) on the interface and no-slip on the rigid bottom (4.14), the set of weakly nonlinear equations (3.7), (3.9), (4.7) and (4.22) will be used to examine the oscillatory motions in water and fluid mud at the leading order, and the time-average effects in the mud layer at the next order.

5. Periodic waves at leading order

Let us first derive the equations coupling the oscillatory displacements of the free surface and the mud/water interface.

https://doi.org/10.1017/jfm.2012.617 Published online by Cambridge University Press

5.1. *Waves in water*

It can be shown that the linearized version of (3.7) and (3.9) admits a solution that is a simple harmonic function of

$$\xi = \frac{1}{\kappa^2}\int^X \frac{\mathrm{d}X}{\sqrt{h(X)}} - t, \tag{5.1}$$

which represents a coordinate moving at the local wave speed. For the nonlinear problem harmonic generation with slowly varying amplitudes is expected, hence we assume

$$\zeta = \frac{1}{2}\sum_{m=-\infty}^{\infty} A_m \mathrm{e}^{\mathrm{i}m\xi} = \frac{1}{2}\sum_{m=1}^{\infty} A_m(X)\mathrm{e}^{\mathrm{i}m\xi} + \text{c.c.} \quad \text{with } A_0 = 0, A_m^* = A_{-m}, \tag{5.2}$$

where c.c. stands for the complex conjugates of the preceding terms. The unknown harmonic amplitudes A_m remain to be determined. Since derivatives with respect to the fast coordinates are transformed according to

$$\frac{\partial}{\partial t} \to -\frac{\partial}{\partial \xi}, \quad \frac{\partial}{\partial x} \to \frac{1}{\sqrt{h}}\frac{\partial}{\partial \xi} + \kappa^2 \frac{\partial}{\partial X}, \tag{5.3}$$

Equations (3.7) and (3.9) for the water layer become,

$$-\frac{\partial \zeta}{\partial \xi} + \delta\frac{\partial \eta}{\partial \xi} + \kappa^2 \frac{\mathrm{d}h}{\mathrm{d}X}\bar{u} + \kappa^2 h\frac{\partial \bar{u}}{\partial X} + \epsilon\frac{\partial \zeta}{\partial \xi}\frac{\bar{u}}{h^{1/2}} + \epsilon\frac{\zeta}{h^{1/2}}\frac{\partial \bar{u}}{\partial \xi} + h^{1/2}\frac{\partial \bar{u}}{\partial \xi} = O(\epsilon\kappa^2) \tag{5.4}$$

$$-\frac{\partial \bar{u}}{\partial \xi} + \frac{\epsilon}{h^{1/2}}\bar{u}\frac{\partial \bar{u}}{\partial \xi} + \kappa^2\frac{\partial \zeta}{\partial X} + \frac{1}{h^{1/2}}\frac{\partial \zeta}{\partial \xi} + \frac{\kappa^2 h}{3}\frac{\partial^3 \bar{u}}{\partial \xi^3} = O(\epsilon\kappa^2). \tag{5.5}$$

The sum of (5.4) and $h^{1/2}\times$ (5.5) leaves only terms of $O(\kappa^2, \delta, \epsilon)$

$$\delta\frac{\partial \eta}{\partial \xi} + \kappa^2\frac{\mathrm{d}h}{\mathrm{d}X}\bar{u} + \kappa^2 h\frac{\partial \bar{u}}{\partial X} + \frac{\epsilon}{h^{1/2}}\frac{\partial \zeta}{\partial \xi}\bar{u} + \frac{\epsilon}{h^{1/2}}\zeta\frac{\partial \bar{u}}{\partial \xi} + h^{1/2}\left(\frac{\epsilon}{h^{1/2}}\bar{u}\frac{\partial \bar{u}}{\partial \xi} + \kappa^2\frac{\partial \zeta}{\partial X} + \frac{\kappa^2 h}{3}\frac{\partial^3 \bar{u}}{\partial \xi^3}\right) = O(\epsilon\kappa^2). \tag{5.6}$$

Now $\bar{u}$ can be eliminated from the two equations above by using the first-order approximation of (5.4) or (5.5):

$$\bar{u} = \frac{\zeta}{h^{1/2}} + O(\epsilon\kappa^2), \quad \frac{\partial \bar{u}}{\partial X} = \frac{1}{h^{1/2}}\frac{\partial \zeta}{\partial X} - \frac{h_X}{2h^{3/2}}\zeta + O(\epsilon\kappa^2), \tag{5.7}$$

yielding finally the following nonlinear equation coupling ζ and η

$$2h^{1/2}\frac{\partial \zeta}{\partial X} + \frac{h_X}{2h^{1/2}}\zeta + \frac{3}{2h}\frac{\epsilon}{\kappa^2}\frac{\partial(\zeta^2)}{\partial \xi} + \frac{h}{3}\frac{\partial^3 \zeta}{\partial \xi^3} = -\frac{\delta}{\kappa^2}\frac{\partial \eta}{\partial \xi} + O(\kappa) \tag{5.8}$$

where all terms are of the same order. This result is simply an extension of the familiar Korteweg–de Vries equation by accounting for the mud layer.

We now assume for the interface displacement,

$$\eta = \frac{1}{2}\sum_{m=-\infty}^{\infty} B_m(X)\mathrm{e}^{\mathrm{i}m\xi} = \frac{1}{2}\sum_{m=1}^{\infty} B_m(X)\mathrm{e}^{\mathrm{i}m\xi} + \text{c.c.} \tag{5.9}$$

with $B_m^* = B_{-m}$ and $B_0 = 0$. By substituting (5.2) and (5.9) into (5.8), a set of nonlinear ordinary differential equations coupling A_m and B_m is derived. In particular

https://doi.org/10.1017/jfm.2012.617 Published online by Cambridge University Press

the quadratic term in (5.8) can be manipulated to be

$$4\zeta^2 = \left(\sum_{\ell=-\infty}^{\infty} A_\ell \mathrm{e}^{\mathrm{i}\ell\xi}\right)^2$$
$$= \sum_{\ell=1}^{\infty}\left\{\mathrm{e}^{\mathrm{i}m\xi}\left[\sum_{\ell=1}^{\infty} 2A_\ell^* A_{m+\ell} + \sum_{\ell=1}^{[m/2]} \alpha_\ell A_\ell A_{m-\ell}\right] + \text{c.c.}\right\} + \sum_{1}^{\infty} A_\ell A_\ell^* \qquad (5.10)$$

where $\alpha_l = 1$ and $\alpha_\ell = 2$ if $\ell = 1, 2, 3, \ldots, m/2 - 1$, and $[m/2]$ denotes the integer part of $m/2$ (see, Rogers & Mei (1978) and Mei (1989, p. 604)).

After using $A_{-m} = A_m^*$, we get, for every positive integer $m = 1, 2, 3, \ldots$,

$$\sqrt{h}\frac{\mathrm{d}A_m}{\mathrm{d}X} + \frac{h_X}{4\sqrt{h}}A_m - \frac{\mathrm{i}m^3}{6}hA_m + \frac{\epsilon}{\kappa^2}\frac{3\mathrm{i}}{8h}m\left[\sum_{l=1}^{\infty} 2A_l^* A_{m+l} + \sum_{l=1}^{[m/2]} \alpha_l A_l A_{m-l}\right]$$
$$+ \frac{\delta}{\kappa^2}\frac{\mathrm{i}m}{2}B_m = 0. \qquad (5.11)$$

Another relation between A_m and B_m is needed and will be found next by examining the leading-order motion of the fluid mud.

5.2. *Leading-order motion of fluid mud*

The momentum equation (4.22) will now be solved by assuming the following two-scale expansions,

$$U = U^{(0)} + \kappa^2 U^{(1)} + \cdots, \quad W = W^{(0)} + \kappa^2 W^{(1)} + \cdots, \quad \tau_{xz} = \tau_{xz}^{(0)} + \kappa^2 \tau_{xz}^{(1)} + \cdots, \qquad (5.12)$$

where $U^{(n)}, W^{(n)}$ and $\tau_{xz}^{(n)}$ are functions of x, X and Z. In stationary coordinates, the mass and momentum conservation laws are, at the leading order ($n = 0$),

$$\frac{\partial U^{(0)}}{\partial x} + \frac{\kappa^2}{\delta}\frac{\mathrm{d}h}{\mathrm{d}X}\frac{\partial U^{(0)}}{\partial Z} + \frac{\partial W^{(0)}}{\partial Z} = 0, \quad 0 < Z < 1; \qquad (5.13)$$

$$\frac{\partial U^{(0)}}{\partial t} - \frac{1}{R}\frac{\partial \tau_{xz}^{(0)}}{\partial Z} = -\gamma\frac{\partial \zeta^{(0)}}{\partial x} \quad 0 < Z < 1. \qquad (5.14)$$

After Taylor expansion about the mean interface at $Z = 1$, the boundary conditions (4.15) and (4.20) on the mean interface are

$$\frac{\partial \eta^{(0)}}{\partial t} = W^{(0)} + \frac{\kappa^2}{\delta}U^{(0)}\frac{\mathrm{d}h}{\mathrm{d}X}, \quad Z = 1 \qquad (5.15)$$

and

$$\frac{\partial U^{(0)}}{\partial Z} = 0, \quad Z = 1. \qquad (5.16)$$

At the rigid bottom we have

$$U^{(0)} = W^{(0)} = 0, \quad Z = 0. \qquad (5.17)$$

https://doi.org/10.1017/jfm.2012.617 Published online by Cambridge University Press

Changing to the moving coordinates according to (5.1), we get from (5.13) and (5.14)

$$\frac{1}{\sqrt{h}}\frac{\partial U^{(0)}}{\partial \xi}+\frac{\kappa^2}{\delta}\frac{\mathrm{d}h}{\mathrm{d}X}\frac{\partial U^{(0)}}{\partial Z}+\frac{\partial W^{(0)}}{\partial Z}=0, \quad 0<Z<1 \tag{5.18}$$

$$\frac{1}{R}\frac{\partial \tau_{xz}^{(0)}}{\partial Z}+\frac{\partial U^{(0)}}{\partial \xi}=\frac{\gamma}{\sqrt{h}}\frac{\partial \zeta^{(0)}}{\partial \xi}, \quad 0<Z<1 \tag{5.19}$$

and from (5.15)

$$-\frac{\partial \eta^{(0)}}{\partial \xi}=W^{(0)}+\frac{\kappa^2}{\delta}\frac{\mathrm{d}h}{\mathrm{d}X}U^{(0)}, \quad Z=1. \tag{5.20}$$

Conditions (5.16) and (5.17) are unchanged.

Let the mud solutions be

$$U^{(0)}=\frac{1}{2}\sum_{m=1}^{\infty}U_m^{(0)}(Z)\mathrm{e}^{\mathrm{i}m\xi}+\text{c.c.}, \quad W^{(0)}=\frac{1}{2}\sum_{m=1}^{\infty}W_m^{(0)}(Z)\mathrm{e}^{\mathrm{i}m\xi}+\text{c.c.} \tag{5.21a}$$

$$\tau_{xz}^{(0)}=\frac{1}{2}\sum_{m=1}^{\infty}(\tau_{xz}^{(0)})_m(Z)\mathrm{e}^{\mathrm{i}m\xi}+\text{c.c.} \tag{5.21b}$$

where the parametric dependence on X is suppressed for brevity. It follows from (5.19) that

$$\frac{1}{R}\frac{\mathrm{d}\,(\tau_{xz}^{(0)})_m}{\mathrm{d}Z}+\mathrm{i}mU_m^{(0)}=\frac{\mathrm{i}m\gamma}{h^{1/2}}A_m, \tag{5.22}$$

for each harmonic. Since

$$(\tau_{xz}^{(0)})_m=\mu_m\frac{\mathrm{d}U_m^{(0)}}{\mathrm{d}Z}+O(\kappa^4) \tag{5.23}$$

where

$$\mu_m\equiv\frac{\mu_c'(m\omega)}{\mu_s}, \tag{5.24}$$

is the dimensionless complex viscosity for the mth harmonic, now (5.22) becomes

$$\frac{\mathrm{d}^2U_m^{(0)}}{\mathrm{d}Z^2}-\sigma_m^2U_m^{(0)}=-\frac{\sigma_m^2\gamma}{h^{1/2}}A_m \tag{5.25}$$

where σ_m is the complex parameter defined by

$$\sigma_m=\sqrt{-\mathrm{i}\frac{mR}{\mu_m}}=\sqrt{-\mathrm{i}\frac{\rho_M m\omega d^2}{\mu_c'(m\omega)}}=\sqrt{2}\frac{d}{\delta_m}\mathrm{e}^{-\mathrm{i}(\theta_m/2+\pi/4)} \tag{5.26}$$

where $\theta_m=\theta(m\omega)$ is independent of the mud-layer thickness d. As shown in figure 3, θ_m is almost constant within 0.1 rad $\mathrm{s}^{-1}\leqslant m\omega\leqslant 10$ rad s^{-1} for both the Hangzhou Bay mud and Lianyun Harbor mud. The quantity δ_m defined by

$$\delta_m=\sqrt{\frac{2|\mu_c'(m\omega)|}{\rho_M m\omega}}. \tag{5.27}$$

is just the Stokes boundary layer thickness at frequency $m\omega$. For the same $m\omega$, δ_m is smaller for the less viscous Hangzhou Bay mud. Since $|\mu_c'(m\omega)|$ decreases with

https://doi.org/10.1017/jfm.2012.617 Published online by Cambridge University Press

increasing $m\omega$, δ_m is smaller for higher frequencies or higher harmonics, hence σ_m is greater for the same mud depth d. Clearly the less viscous mud from Hangzhou Bay has much greater $|\sigma_m|$. Note that σ_m does not depend on the scale μ_s, whose choice is therefore immaterial in later computations.

The solution for $U_m^{(0)}$ satisfying the no-slip condition (5.17) at the bottom and the shear-free condition (5.16) at $Z = 1$ is

$$U_m^{(0)} = \frac{\gamma A_m}{\sqrt{h}} \left[1 - \cosh(\sigma_m Z) + \tanh(\sigma_m) \sinh(\sigma_m Z)\right]. \tag{5.28}$$

From (5.18), we also have

$$\frac{\partial W_m^{(0)}}{\partial Z} = -\frac{\mathrm{i}m}{\sqrt{h}} U_m^{(0)} - \frac{\kappa^2}{\delta} \frac{\mathrm{d}h}{\mathrm{d}X} \frac{\partial U_m^{(0)}}{\partial Z}. \tag{5.29}$$

Using the no-slip boundary condition on the bottom, we obtain

$$\begin{aligned} W_m^{(0)} = {} & -\mathrm{i}m \frac{\gamma A_m}{\sigma_m h} \{\sigma_m Z - \sinh(\sigma_m Z) + \tanh(\sigma_m) \cosh(\sigma_m Z) - \tanh(\sigma_m)\} \\ & - \frac{\kappa^2}{\delta} \frac{\mathrm{d}h}{\mathrm{d}X} U_m^{(0)}. \end{aligned} \tag{5.30}$$

On the top of the mud layer, condition (5.20) now requires

$$B_m(X) = -\frac{1}{\mathrm{i}m} \left(W_m^{(0)} + \frac{\kappa^2}{\delta} \frac{\mathrm{d}h}{\mathrm{d}X} U_m^{(0)} \right), \quad Z = 1. \tag{5.31}$$

After using (5.28) and (5.30), we obtain

$$B_m(X) = \frac{\gamma A_m}{h} \left(1 - \frac{\tanh \sigma_m}{\sigma_m}\right) \equiv \frac{\gamma A_m}{h} \mathscr{G}(\sigma_m) \tag{5.32}$$

for $m = 1, 2, \ldots,$ which gives the ratio of the free surface and the interface harmonics. Note that the bed slope does not appear explicitly.

The factor

$$\mathscr{G}(\sigma_m) = 1 - \frac{\tanh \sigma_m}{\sigma_m} \tag{5.33}$$

characterizes the wave/mud interaction and is identical in form to $G(\sigma)$ for monochromatic waves in Mei *et al.* (2010). The modulus $|\mathscr{G}(\sigma_m)|$ is essentially the amplitude ratio of interface to free surface for the mth harmonic. It will be shown shortly that $\mathrm{Im}(\mathscr{G}(\sigma_m))$ is responsible for energy transfer from surface waves to mud. Using the reasoning of Mei *et al.* (2010), it can be shown that for $|\sigma_m| \gg 1$, i.e. very small viscosity $|\mu_c|$, large m or deep mud, $\mathscr{G} \approx 1$ hence almost real; damping is weak and the interface and free surface oscillate in phase. On the other hand, for $|\sigma_m| \ll 1$, i.e. a highly viscous or shallow mud, $|\mathscr{G}| \ll 1$, the mud layer hardly moves. It was also shown by Mei *et al.* (2010) that in the strictly elastic limit when

$$\theta_m = \frac{\pi}{2} \quad \text{and} \quad |\sigma_m| = \sqrt{2} \frac{d}{\delta_m} = \left(\frac{1}{2} + n\right) \pi \tag{5.34}$$

the magnitude of $\mathscr{G}$ becomes unbounded and resonance occurs, a feature first noted by Ng & Zhang (2007) using the Kelvin–Voigt model with two constant

https://doi.org/10.1017/jfm.2012.617 Published online by Cambridge University Press

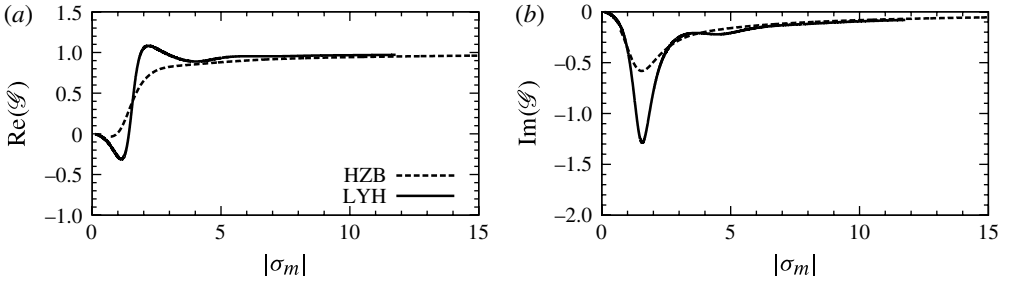


FIGURE 4. Variations of real (a) and imaginary (b) parts of $\mathscr{G}(\sigma_m)$ with $|\sigma_m|$ for the Hangzhou Bay mud (HZB) and Lianyun Harbor mud (LYH).

coefficients. Near-resonance can occur for large enough mud depth or high enough frequency. For our two types of mud, θ_m varies only modestly over a wide range of frequencies. The real and imaginary parts of $\mathscr{G}(\sigma_m)$ are primarily affected by $|\sigma_m|$, as shown in figure 4. It will be shown in § 6.2 that the attenuation rate of the mth harmonic component is proportional to the imaginary part of $m\mathscr{G}(\sigma_m)$. The fact that $\mathrm{Im}(\mathscr{G}(\sigma_m))$ is negative implies of course wave damping, which is the strongest when $\mathrm{Im}(\mathscr{G}(\sigma_m))$ is a local minimum. Hence attenuation is more severe in the Lianyun Harbor mud.

For a given mud, $|\sigma_m|$ changes with the mud-layer thickness d and the wave frequency $m\omega$. Numerical examples will be presented shortly for $\omega = 0.4398$ rad s^{-1}. Correspondingly values of $m\mathscr{G}(\sigma_m)$ are shown in figure 5 for the first 10 harmonics and 3 mud-layer thicknesses $d = 0.50, 0.75, 1.0$ m. For the Hangzhou Bay mud the values of $|\sigma_m|$ are all greater than that at the resonance peak shown in figure 4. For the Lianyun Harbor mud the peak is surrounded by the first few values of $|\sigma_m|$, $m = 1, 2, 3, 4$ shown in figure 5. Thus, under the same wave conditions, resonance must play an important role in the attenuation for the Lianyun Harbor mud, but not for the Hangzhou Bay mud.

6. Evolution of surface-wave harmonics

6.1. *The evolution equation*

Eliminating B_m from (5.11) by using (5.32), we finally obtain the nonlinear system for A_m

$$\sqrt{h}\frac{\mathrm{d}A_m}{\mathrm{d}X} + \frac{h_X}{4\sqrt{h}}A_m - \frac{\mathrm{i}m^3}{6}hA_m + \frac{\epsilon}{\kappa^2}\frac{3\mathrm{i}}{8h}m\left[\sum_{l=1}^{\infty} 2A_l^* A_{m+l} + \sum_{l=1}^{[m/2]} \alpha_l A_l A_{m-l}\right] + \frac{\mathrm{i}m}{2}\frac{\delta}{\kappa^2}\frac{\gamma A_m}{h}\left[1 - \frac{\tanh\sigma_m}{\sigma_m}\right] = 0, \quad m = 1, 2, 3, \ldots. \tag{6.1}$$

Since

$$\sqrt{h}\frac{\mathrm{d}A_m}{\mathrm{d}X} + \frac{h_X}{4\sqrt{h}}A_m = h^{1/4}\frac{\mathrm{d}(h^{1/4}A_m)}{\mathrm{d}X}. \tag{6.2}$$

https://doi.org/10.1017/jfm.2012.617 Published online by Cambridge University Press

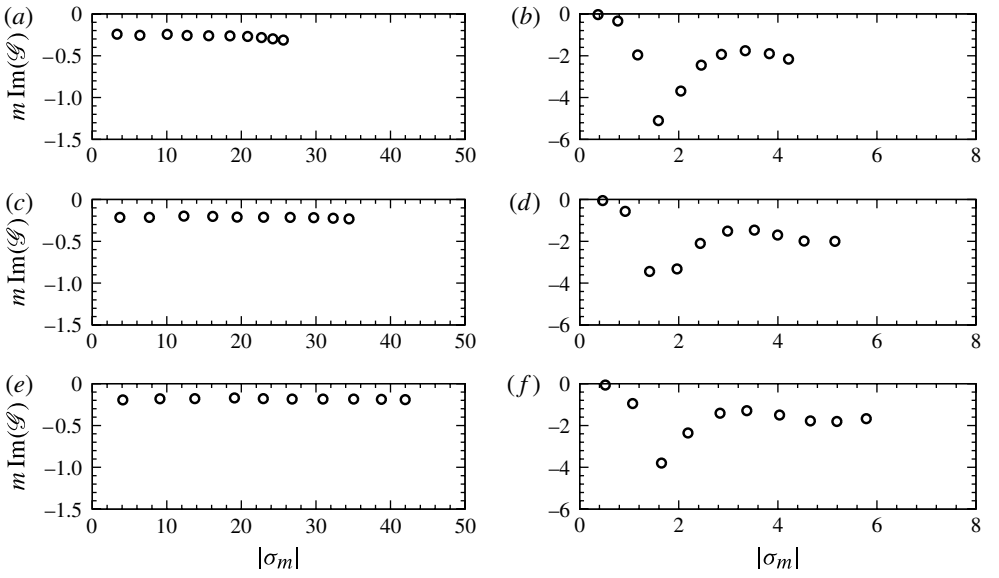


FIGURE 5. Contrast between Hangzhou Bay mud (*a,c,e*) and Lianyun Harbor mud (*b,d,f*) for $m\mathrm{Im}\mathscr{G}(\sigma_m)$ as a function of $|\sigma_m| = d\sqrt{2/\delta_m}$ for $m = 1, 2, 3\ldots, 10$ at the same frequency $\omega = 0.4398$ rad s^{-1}. From top to bottom row, the mud depths are $d = 0.50$, 0.75 and 1.00 cm, respectively. Each symbol corresponds to a value of m, increasing from left ($m = 1$) to right ($m = 10$).

Equation (6.1) can be rewritten as

$$\frac{\mathrm{d}(h^{1/4}A_m)}{\mathrm{d}X} - \frac{\mathrm{i}m^3}{6}h^{3/4}A_m + \frac{\epsilon}{\kappa^2}\frac{3\mathrm{i}}{8h^{5/4}}m\left[\sum_{l=1}^{\infty} 2A_l^*A_{m+l} + \sum_{l=1}^{[m/2]}\alpha_l A_l A_{m-l}\right] + \frac{\delta}{\kappa^2}\frac{\mathrm{i}\gamma}{2h^{5/4}}m\left[1 - \frac{\tanh(\sigma_m)}{\sigma_m}\right]A_m = 0. \tag{6.3}$$

For $h =$ constant and $\delta = 0$, the reduced system appears in nonlinear optics, and also in long waves in a shallow sea with a rigid and smooth bottom (Mei & Ünlüata 1972; Bryant 1976). With a different coefficient in the last term, the equation also governs long waves suffering incoherent scattering by a randomly rough seabed (Grataloup & Mei 2003). After truncation this nonlinear system can be solved numerically by finite differences for given $A_m(0)$ by marching in X from $X = 0$. The interface harmonics B_m then follow from (5.32).

6.2. *Energy attenuation*

Denoting for brevity $\widehat{A}_m = h^{1/4}A_m$, we rewrite (6.3) as

$$\frac{\mathrm{d}\widehat{A}_m}{\mathrm{d}X} - \frac{\mathrm{i}m^3}{6}h^{1/2}\widehat{A}_m + \frac{3\mathrm{i}}{8}\frac{\epsilon}{\kappa^2}m\frac{1}{h^{7/4}}\left(\sum_{l=1}^{\infty} 2\widehat{A}_l^*\widehat{A}_{m+l} + \sum_{l=1}^{[m/2]}\alpha_l\widehat{A}_l\widehat{A}_{m-l}\right) + \frac{1}{h^{3/2}}\frac{\delta}{\kappa^2}\frac{\mathrm{i}\gamma}{2}m\left(1 - \frac{\tanh(\sigma_m)}{\sigma_m}\right)\widehat{A}_m = 0. \tag{6.4}$$

https://doi.org/10.1017/jfm.2012.617 Published online by Cambridge University Press

By multiplying the above equation by $\widehat{A}_m^*$, summing over m, and adding the result equation to its complex conjugate, an energy equation can be derived. In their study of long-wave scattering by a randomly rough seabed, Grataloup & Mei (2003) have shown by mathematical induction that the nonlinear terms of the same form in (6.4) disappears, hence

$$\frac{\mathrm{d}}{\mathrm{d}X}\left[\sum_{m=1}^{n}\left|\widehat{A}_m\right|^2\right] = -2\frac{1}{h^{3/2}}\frac{\delta}{\kappa^2}\sum_{m=1}^{n}\mathrm{Im}\left[\frac{\gamma}{2}m\left(1-\frac{\tanh(\sigma_m)}{\sigma_m}\right)\right]\left|\widehat{A}_m\right|^2 \tag{6.5}$$

or

$$\frac{\mathrm{d}}{\mathrm{d}X}\left[\sqrt{h}\sum_{m=1}^{n}\left|A_m\right|^2\right] = \frac{\gamma}{h}\frac{\delta}{\kappa^2}\sum_{m=1}^{n}\mathrm{Im}\left[m\left(1-\frac{\tanh(\sigma_m)}{\sigma_m}\right)\right]\left|A_m\right|^2. \tag{6.6}$$

Since $\sqrt{h}$ is the dimensionless group velocity of long waves, the spatial rate of total energy decay is proportional to $\mathrm{Im}\left[m\mathscr{G}(\sigma_m)\right]$, and unaffected by nonlinearity which only contributes to energy exchange among different harmonics. Equation (6.6) will be used to check the accuracy of numerical computations.

6.3. *Behaviour at the shore line*

As waves approach the shore dissipation must increase so that all harmonics of the free surface and the interface must diminish in magnitude. At some station X_0 close to shore nonlinear coupling is no longer important, so that only the linear terms in (6.4) matter. Equivalently, (6.6) can be simplified by keeping just the mth term in the series. Denoting for brevity

$$\frac{\alpha_m}{h} = -\frac{\gamma}{h}\frac{\delta}{\kappa^2}\mathrm{Im}\left[m\left(1-\frac{\tanh(\sigma_m)}{\sigma_m}\right)\right] \tag{6.7}$$

we have

$$\frac{\mathrm{d}}{\mathrm{d}X}\left[\sqrt{h}\left|A_m\right|^2\right] \approx -\frac{\alpha_m}{h}\left|A_m\right|^2 = -\frac{\alpha_m}{h^{3/2}}\sqrt{h}\left|A_m\right|^2, \quad X_0 < X < X_s \tag{6.8}$$

where X_s designates the shoreline. Let the beach be approximated locally as a plane so that

$$h(X) = s(X_s - X) \quad \text{with } s = \frac{h(X_0)}{X_s - X_0} \tag{6.9}$$

where X_0 is slightly less than X_s. It follows after integration that

$$\frac{|A_m(X)|^2}{|A_m(X_0)|^2} = \sqrt{\frac{h(X_0)}{h(X)}}\frac{\exp\left(\dfrac{2\alpha_m}{s\sqrt{h(X_0)}}\right)}{\exp\left(\dfrac{2\alpha_m}{s\sqrt{h(X)}}\right)}. \tag{6.10}$$

Since $\alpha_m > 0$ and $h^{-1/2} \to \infty$ as $X \to X_s$, $|A_m|^2$ diminishes to zero exponentially fast towards the shoreline. Thus, Green's law is modified: amplitude growth is overshadowed by dissipation. Since when $h \to 0$ the assumption of $d/h \ll 1$ no longer holds and the Boussinesq approximation loses its validity, this result cannot be quantitatively reliable. Nevertheless the predicted trend here is consistent with observations by Wells (1978).

https://doi.org/10.1017/jfm.2012.617 Published online by Cambridge University Press

7. Numerical results of wave evolution

We now examine the evolution of waves over two geometrically identical beaches covered by two types of fluid mud from Hangzhou Bay and Lianyun Harbor, China. In a laboratory test for water/mud mixtures from Zhongshan Harbor, China (Huhe, Huang & Chi 1996), thin layers of mud of densities $\rho_M = 1337$–1510 kg m^{-3} were found to be moved by relatively weak waves (mixture depth = 3 cm, water depths $h = 16$ and 20 cm, wave amplitude = 2.0–2.9 cm and wave period = 1 s). Still denser mixtures can be fluidized by the much stronger waves in nature. In all numerical examples here the fluid density is chosen to be $\rho_M = 1590$ kg m^{-3}. The water depth is given by $h(X) = 1 - sX$, $0 < X < X_s = 1/s$ and $h = 1$, $X < 0$. The mud depth d is constant. Rheological information is taken from figures 2 and 3. In view of the early theories for a rigid and horizontal bed (Mei & Ünlüata 1972; Bryant 1976), generation of higher harmonics and subsequent energy exchanges are expected. In a real sea or in a laboratory experiment, the incident wave energy is exchanged among many harmonics before reaching the beach, so that the amplitude spectrum at $X = 0$ can be complex, depending on the offshore climate and the bathymetry. For physical insight we consider only the simplest initial data with one harmonic $A_1(0) \neq 0$ at the foot of the beach. Thus, the initial values are $A_1(0) = 1$, $A_n(0) = 0$, $n = 1, 2, \ldots$. Numerical solutions of (6.1) have been carried out by finite differences for the first 10 harmonics A_m, $m = 1, 2, \ldots, 10$, after testing with more harmonics for convergence. The computational domain covers the entire beach which is assumed to be plane. The intensity of this nonlinear process should now be accentuated by the decreasing depth but counteracted by dissipation. Because the wavelength of the 10th harmonic decreases as $\sqrt{h(X)}/10$, it was found necessary to use very fine steps close to the shoreline. All our computations are terminated at a short distance before the shoreline. In all computations, numerical accuracy is confirmed by checking with (6.6). Validation tests were first performed for the rigid bed without mud. Owing to the simple assumption of constant mud depth all of the way to the shore, predictions close to the shoreline can at best be of qualitative value.

Consider first a mildly sloping beach with the following physical dimensions: offshore depth $h_0 = 5$ m at $X = 0$, mud-layer depth $d = 0.75$ m. The fundamental frequency of the incident wave is $\omega = 0.4398$ rad s^{-1} (i.e. wave period $T = 14.28$ s) and the amplitude is $A_1 = 0.5$ m. The dimensionless parameters are $\kappa^2 = (kh_0)^2 = (\omega h_0)^2 / g h_0 = 0.0986$, $\delta = 0.15$ and $\epsilon = 0.1$. In physical units, the beach slope $\mathrm{d}h'/\mathrm{d}x'$ is related to the dimensionless slope s by

$$\frac{\mathrm{d}h'}{\mathrm{d}x'} = kh_0 \frac{\mathrm{d}h}{\mathrm{d}x} = (kh_0)^3 \frac{\mathrm{d}h}{\mathrm{d}X} = \kappa^3 s. \tag{7.1}$$

We first select the dimensionless beach slope to be $s = 0.2$, corresponding to the physical slope of 0.006 19 and to beach width = 807.5 m. The harmonics of the surface and the interface are shown in figures 6 and 7. Harmonic generation due to nonlinearity and energy transfer from higher harmonics to the fundamental harmonic are evident across the more Newtonian and less viscous beach covered by Hangzhou Bay mud. On the other hand, dissipation overwhelms nonlinearity for the higher harmonics over the Lianyun Harbor mud. Hence, energy transfer from higher harmonics to the fundamental wave is weak; the interface motion is similarly subdued, consistent with figure 5. The difference is due to the difference in resonance. Near the shoreline where nonlinearity is weakened, the approximation given by (6.10) is compared with the numerical results in figure 8 for the same two beaches in the range $4.8 < X < 5$; the agreement is fairly good for both beaches. Note that for

https://doi.org/10.1017/jfm.2012.617 Published online by Cambridge University Press

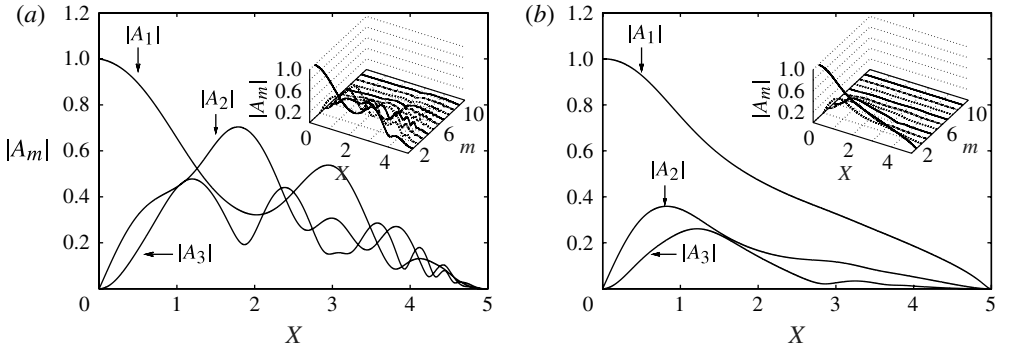


FIGURE 6. Spatial variation of the first few surface harmonics over a gentle beach with $s = 0.2$, for $\epsilon = 0.1$, $\delta = 0.15$, $\kappa^2 = 0.0986$. The incident wave is simple harmonic: $A_1(0) = 1$ and $A_m(0) = 0$ for $m = 2, 3, 4, \ldots$. (*a*) Hangzhou Bay mud. (*b*) Lianyun Harbor mud. The first 10 harmonics are shown in the inset.

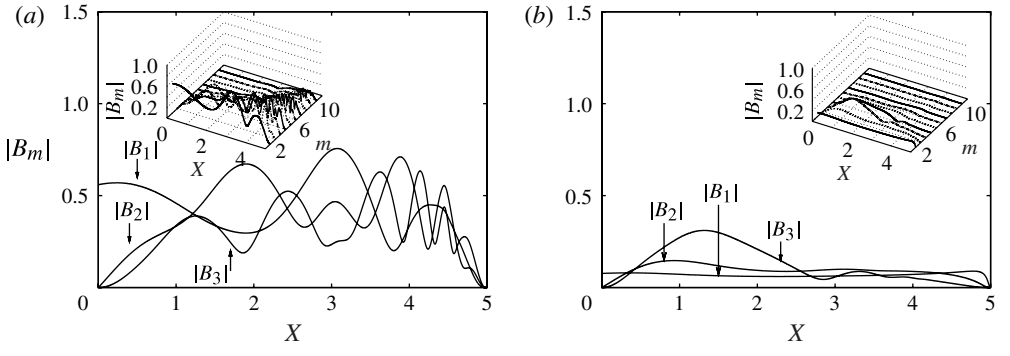


FIGURE 7. Spatial variation of the first few interface harmonics over a gentle beach with $s = 0.2$, for $\epsilon = 0.1$, $\delta = 0.15$, $\kappa^2 = 0.0986$. The incident wave is simple harmonic: $A_1(0) = 1$, $A_m(0) = 0$, $m = 2, 3, 4, \ldots$. (*a*) Hangzhou Bay mud. (*b*) Lianyun Harbor mud. The first 10 harmonics are shown in the inset.

Hangzhou Bay mud, $B_1(X)$ diminishes to zero very abruptly near $X = X_s = 5$ so that the analytical approximation gives at best the qualitative trend.

The effects of stronger waves can be readily anticipated. For illustration let the incident wave amplitude be increased by 50 % so that $\epsilon = 0.15$, with all other parameters kept the same as in figures 6 and 7. As can be seen in figures 9 and 10, the spatial modulation of harmonics due to nonlinearity is now more vigorous over both beaches.

We have also examined the effects of different beach slopes while other parameters are kept unchanged from figures 6 and 7. For a beach with $s = 0.1$, the variations of free-surface and interface harmonics are qualitatively similar, as shown in figures 11 and 12. Since waves give up energy over a longer stretch of mud, the harmonic amplitudes are well diminished further away from the shoreline. For a steeper beach with $s = 0.4$, many more harmonics are generated and exchange their energy vigorously within relatively shorted distances. The interface amplitudes remain significant until very close to the shoreline. These numerical predictions exceed the

https://doi.org/10.1017/jfm.2012.617 Published online by Cambridge University Press

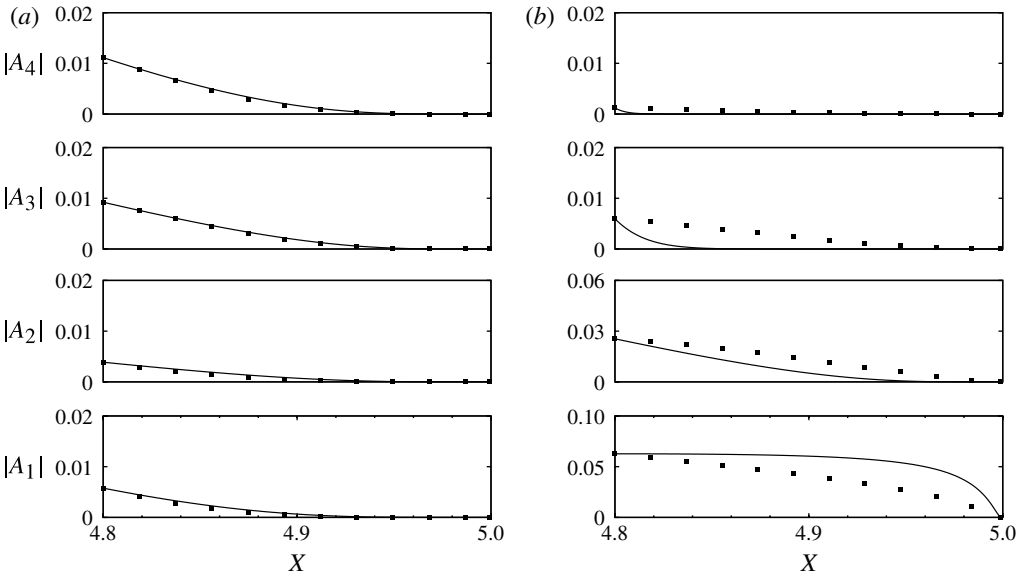


FIGURE 8. The first four surface harmonics near the shoreline for (*a*) Hangzhou Bay mud and (*b*) Lianyun Harbor mud. Solid lines: analytical approximation; squares: numerical results. Inputs are the same as in figures 6 and 7.

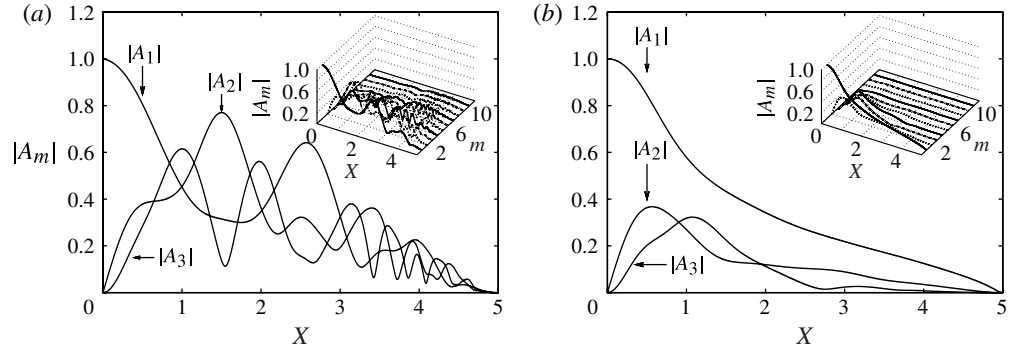


FIGURE 9. Spatial variation of first three surface harmonics for stronger waves with $\epsilon = 0.15$, $\delta = 0.15$, $s = 0.2$, $\kappa^2 = 0.0986$: (*a*) Hangzhou Bay mud; (*b*) Lianyun Harbor mud.

realm of validity of the weakly nonlinear theory. They can only be taken as an indication of the qualitative trend, hence results are not presented here.

8. Steady displacement of fluid mud

8.1. *Mud layer at rest under gravity*

As indicated in figure 2, the dimensional shear modulus $G'(\omega')$ tends towards a finite constant G'_0 as $\omega \to 0$. This is consistent with measurements for static loadings by Huang *et al.* (1992). It is known that a viscoelastic material of Kelvin–Voigt type

https://doi.org/10.1017/jfm.2012.617 Published online by Cambridge University Press

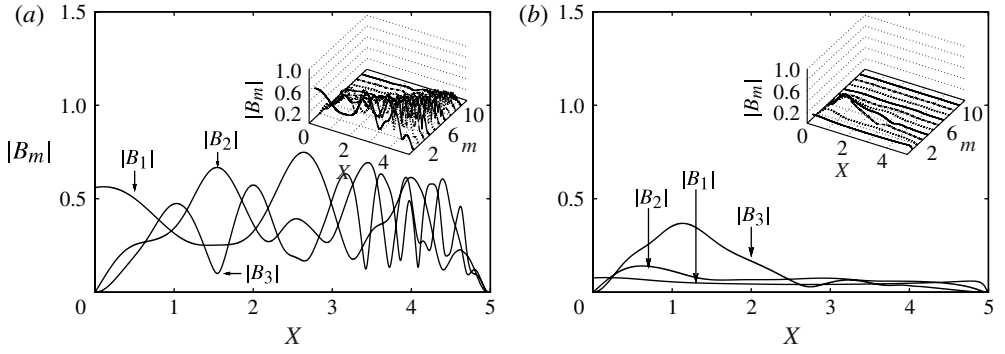


FIGURE 10. Spatial variation of interface harmonics on a sloping beach for stronger waves with $\epsilon = 0.15$, $\delta = 0.15$, $s = 0.2$, $\kappa^2 = 0.0986$: (*a*) Hangzhou Bay mud; (*b*) Lianyun Harbor mud.

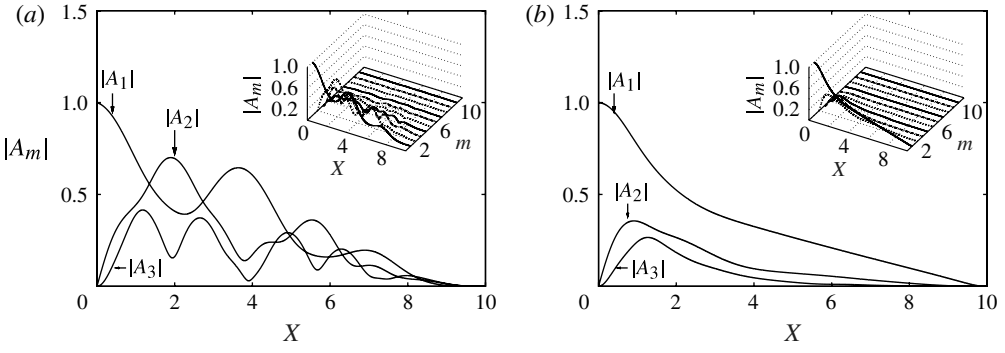


FIGURE 11. Spatial variation of first three surface harmonics on a very gentle beach with $s = 0.1$, for $\epsilon = 0.1$, $\delta = 0.15$, $\kappa^2 = 0.0986$: (*a*) Hangzhou Bay mud; (*b*) Lianyun Harbor mud.

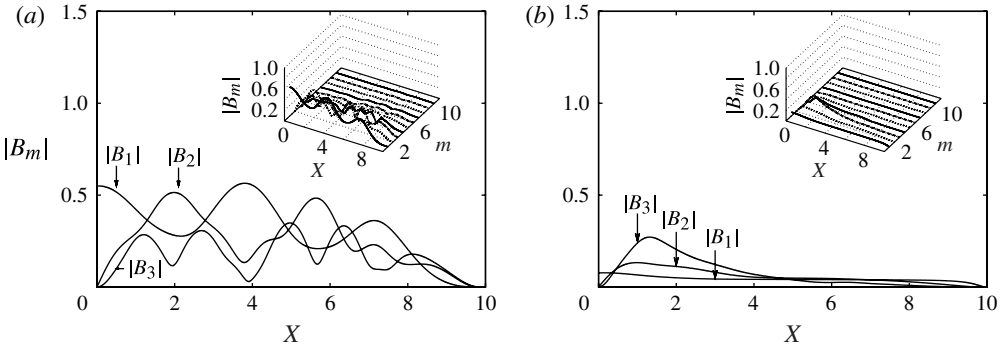


FIGURE 12. Spatial variation of interface harmonics on a very gentle beach with $s = 0.1$, for $\epsilon = 0.1$, $\delta = 0.15$, $\kappa^2 = 0.0986$: (*a*) Hangzhou Bay mud; (*b*) Lianyun Harbor mud.

https://doi.org/10.1017/jfm.2012.617 Published online by Cambridge University Press

modelled by a spring and a damper in parallel can rest on a slope without flow. Referring to figure 1, let $\mathscr{U}'$ denote the horizontal displacement and Z' the vertical coordinate measured from the rigid bottom, as defined by (4.4). For small beach slope $s = \tan\alpha \approx \sin\alpha$, the Z' axis is approximately normal to the bed and $\mathscr{U}'$ is nearly the displacement parallel to the seabed. Balance of tangential forces requires, approximately,

$$-(\rho_M - \rho)gs + G_0' \frac{\mathrm{d}\mathscr{U}'}{\mathrm{d}Z'} \approx 0 \tag{8.1}$$

where $G_0' = G'(0)$ is the static shear modulus. The tangential displacement is

$$\mathscr{U}'(Z') = \frac{(\rho_M - \rho)gs}{2G_0'} Z'(Z' - 2d). \tag{8.2}$$

At the interface, the maximum displacement is $\mathscr{U}'(d) = -(\rho_M - \rho)gsd^2/2G_0'$ which is proportional to the bed slope and to the square of the mud depth.

8.2. *Wave-induced mud displacement*

In a Newtonian fluid, it is well known that there is a steady drift current in the oscillatory boundary layer due to Reynolds stresses originated from convective inertia. In coastal sea waves such a current is important to sediment transport, which may affect the geomorphology of a sandy shore. In the viscoelastic mud layer over a sloping beach, a steady horizontal displacement can be similarly produced by waves. A theoretical analysis of the mean displacement in a horizontal layer of pure mud under a wave-like surface pressure has been studied by Zhang & Ng (2006).

Assuming the expansions (5.12), we get from (4.22) at order $O(\epsilon, \kappa^2)$,

$$-\frac{\partial U^{(1)}}{\partial \xi} - \frac{1}{R}\frac{\partial \tau_{xz}^{(1)}}{\partial Z} = \frac{\gamma}{\sqrt{h}}\frac{\partial}{\partial \xi}\left(\zeta^{(1)} - \frac{\delta}{\kappa^2}\eta^{(0)}\right) - \gamma\frac{\partial \zeta^{(0)}}{\partial X} - \frac{\epsilon}{\kappa^2}\left[\frac{1}{\sqrt{h}}U^{(0)}\frac{\partial U^{(0)}}{\partial \xi} + \left(W^{(0)} + \frac{\kappa^2}{\delta}\frac{\mathrm{d}h}{\mathrm{d}X}U^{(0)}\right)\frac{\partial U^{(0)}}{\partial Z}\right]. \tag{8.3}$$

Taylor expansion of (4.20) around $Z = 1$ gives the boundary condition

$$\tau_{xz}^{(1)} = -\frac{\epsilon}{\kappa^2}\eta\frac{\partial \tau_{xz}^{(0)}}{\partial Z} + O(\epsilon^2), \quad Z = 1. \tag{8.4}$$

In general, $U^{(1)}$ and $\tau_{xz}^{(1)}$ consist of an infinite number of harmonics. The non-zero harmonics are minor corrections to the leading-order velocity $U^{(0)}$. Let us therefore examine only the zeroth harmonic which first appears at the order $O(\epsilon)$ and affects the bed morphology in the long run.

Denoting the time average, i.e. the period average of F with respect to ξ by $\langle F\rangle$, we get from (8.3),

$$\frac{1}{R}\frac{\partial \langle\tau_{xz}^{(1)}\rangle}{\partial Z} = \frac{\epsilon}{\kappa^2}\left\langle \frac{\kappa^2}{\delta}\frac{\mathrm{d}h}{\mathrm{d}X}U^{(0)}\frac{\partial U^{(0)}}{\partial Z} + W^{(0)}\frac{\partial U^{(0)}}{\partial Z}\right\rangle. \tag{8.5}$$

Use has been made of the fact that $\langle\zeta^{(0)}\rangle = 0$ and the averages of all derivatives with respect to ξ are zero due to periodicity.

https://doi.org/10.1017/jfm.2012.617 Published online by Cambridge University Press

The mean shear stress $\langle \tau_{xz}^{(1)} \rangle = (\tau_{xz}^{(1)})_0$ is related to the steady strain by

$$\langle \tau_{xz}^{(1)} \rangle = (\tau_{xz}^{(1)})_0 = G_0 \frac{\partial \mathscr{U}_0^{(1)}}{\partial Z} + O(\kappa^4) \tag{8.6}$$

where $\mathscr{U}_0^{(1)}$ is the steady mud displacement in the horizontal direction and G_0 is the dimensionless shear modulus related to its physical counterpart G_0' by

$$G_0 = \frac{G_0'}{(\mu_s k \sqrt{g h_0})}. \tag{8.7}$$

After using (8.6) and (5.21) in (8.5), we obtain

$$\frac{\partial^2 \mathscr{U}_0^{(1)}}{\partial Z^2} = \frac{1}{2} \frac{\epsilon R}{\kappa^2 G_0} \sum_{m=1}^{\infty} \mathrm{Re} \left[\left(W_{-m}^{(0)} + \frac{\kappa^2}{\delta} \frac{\mathrm{d}h}{\mathrm{d}X} U_{-m}^{(0)} \right) \frac{\partial U_m^{(0)}}{\partial Z} \right]. \tag{8.8}$$

Note that R/G_0 does not depend on the normalization constant μ_s. Substituting (5.28) and (5.30) into the right-hand side gives the following differential equation for $\mathscr{U}_0^{(1)}$

$$\frac{\partial^2 \mathscr{U}_0^{(1)}}{\partial Z^2} = -\frac{1}{2} \frac{\epsilon R}{\kappa^2 G_0} \frac{\gamma^2}{h^{3/2}} \sum_{m=1}^{\infty} \mathrm{i}m \, |A_m|^2 \, \mathrm{Re} \{ F_m(\sigma_m, Z) \}, \quad 0 < Z < 1 \tag{8.9}$$

where

$$\begin{aligned} F_m(\sigma_m, Z) = \frac{\sigma_m}{\sigma_{-m}} \{ & [\sigma_{-m} Z - \sinh(\sigma_{-m} Z) + \tanh(\sigma_{-m})(\cosh(\sigma_{-m} Z) - 1)] \\ & \times [-\sinh(\sigma_m Z) + \tanh(\sigma_m) \cosh(\sigma_m Z)] \}, \quad 0 < Z < 1 \end{aligned} \tag{8.10}$$

with $\sigma_{-m} \equiv \sigma_m^*$. Equation (8.9) must be supplemented by the no-slip condition on the seabed,

$$\mathscr{U}_0^{(1)} = 0, \quad Z = 0. \tag{8.11}$$

On the interface, we use the zeroth harmonic of (8.4),

$$\left(\tau_{xz}^{(1)} \right)_0 = -\frac{\epsilon}{\kappa^2} \left(\eta^{(0)} \frac{\partial \tau_{xz}^{(0)}}{\partial Z} \right)_0, \quad Z = 1. \tag{8.12}$$

Let

$$\tau_{xz}^{(0)} = \frac{1}{2} \sum_{m=1}^{\infty} \left(\tau_{xz}^{(0)} \right)_m \mathrm{e}^{\mathrm{i}m\xi} + \mathrm{c.c.} = \frac{1}{2} \sum_{m=1}^{\infty} \mu_m \frac{\partial U_m^{(0)}}{\partial Z} \mathrm{e}^{\mathrm{i}m\xi} + \mathrm{c.c.} \tag{8.13}$$

where μ_m is the normalized complex viscosity at the frequency $m\omega$,

$$\mu_m \equiv \frac{\mu_c(m\omega)}{\mu_s}. \tag{8.14}$$

With the harmonic expansion for η in (5.9), the interface condition (8.12) can be reduced to

$$\begin{aligned} G_0 \frac{\mathrm{d}\mathscr{U}_0^{(1)}}{\mathrm{d}Z} \bigg|_{Z=1} &= -\frac{1}{2} \frac{\epsilon}{\kappa^2} \mathrm{Re} \sum_{m=1}^{\infty} \mu_m B_{-m} \frac{\mathrm{d}^2 U_m^{(0)}}{\mathrm{d}Z^2} \\ &= -\frac{1}{2} \frac{\epsilon}{\kappa^2} \mathrm{Re} \sum_{m=1}^{\infty} \mu_m A_{-m} \mathscr{G}(\sigma_m) \frac{\mathrm{d}^2 U_m^{(0)}}{\mathrm{d}Z^2}, \quad Z = 1, \end{aligned} \tag{8.15}$$

https://doi.org/10.1017/jfm.2012.617 Published online by Cambridge University Press

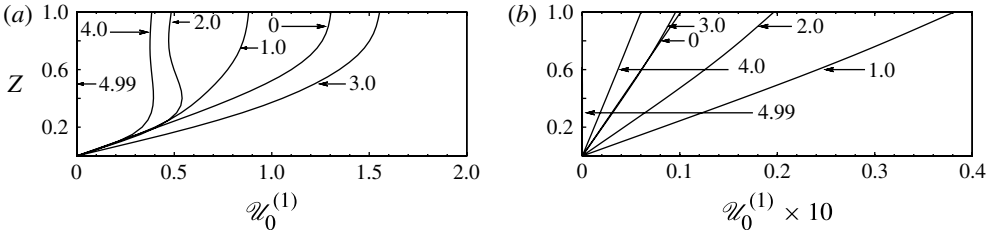


FIGURE 13. Vertical profiles of mean interface displacement at selected stations ($X = 0, 1, 2, 3, 4, 4.99$) for Hangzhou Bay mud (*a*), $\mathscr{U}_0^{(1)}$ and Lianyun Harbor mud (*b*), $10 \times \mathscr{U}_0^{(1)}$. Inputs are the same as in figures 6 and 7.

where $\mathscr{G}(\sigma_m)$ is defined in (5.33). From the solution (5.28) for $U_m^{(0)}$, we find

$$\frac{\mathrm{d}^2 U_m^{(0)}}{\mathrm{d}Z^2} = \frac{\gamma A_m}{\sqrt{h}} \sigma_m^2 \operatorname{sech}(\sigma_m), \quad Z = 1, \tag{8.16}$$

which is then used to give the interface condition

$$\left.\frac{\mathrm{d}\mathscr{U}_0^{(1)}}{\mathrm{d}Z}\right|_{Z=1} = \frac{1}{2}\frac{\epsilon\gamma}{\kappa^2 G_0 h^{3/2}} \sum_{m=1}^{\infty} |A_m|^2 \operatorname{Re}\left[\mathscr{G}(\sigma_m)\sigma_{-m}{}^2 \mu_{-m} \operatorname{sech}(\sigma_{-m})\right]. \tag{8.17}$$

It is straightforward to integrate (8.9) subject to (8.11) and (8.17) to get the drift displacement

$$\mathscr{U}_0^{(1)} = Z \left.\frac{\mathrm{d}U_0^{(1)}}{\mathrm{d}Z}\right|_{Z=1} + \frac{\epsilon R}{\kappa^2 G_0}\frac{\gamma^2}{h^{3/2}} \operatorname{Re}\left\{\sum_{m=1}^{\infty} \mathrm{i}m\,|A_m|^2 \int_0^Z \mathrm{d}Z' \int_1^{Z'} \mathrm{d}Z'' F_m(\sigma_m, Z'')\right\}. \tag{8.18}$$

The lengthy analytical expression of the double integral is recorded in Appendix.

We point out that the second-order drift displacement is the result of nonlinear forcing by quadratic products of the first-order deformation which is predicted by the linear law of viscoelasticity. Since no measured data are available for the shear modulus at the limit of $\omega = 0$, a crude estimate is made by extrapolating the mud data in figure 2. The results are $G_0' = 9.6$ Pa for the Hangzhou Bay mud and $G_0' = 967$ Pa for the Lianyun Harbor mud.

Figure 13 shows the calculated mean mud displacements at selected stations. It can be seen that the depth profile is much more linear layer for the Lianyun Harbor mud. Figure 14 shows the spatial variation of the mud drift on the interface. The horizontal variation across the beach is relatively mild compared with the variation of B_m, and is very small in the more elastic mud of Lianyun Harbor. The displacement is especially small at $X = 0$ due to the smallness of $\mathscr{G}(\sigma_m)$ and little mud motion there.

From the period average of the incompressibility condition (4.7) we get at the second order

$$-\frac{\kappa^2}{\delta}\frac{\mathrm{d}h}{\mathrm{d}X}\frac{\partial \mathscr{U}_0^{(1)}}{\partial Z} + \frac{\partial \mathscr{W}_0^{(1)}}{\partial Z} = 0, \quad 0 < Z < 1. \tag{8.19}$$

Upon integration the second-order vertical displacement of the interface $\mathscr{W}_0^{(1)}(X, 1)$ is found:

$$\mathscr{W}_0^{(1)}(X, 1) = \frac{\kappa^2}{\delta}\frac{\mathrm{d}h}{\mathrm{d}X}\mathscr{U}_0^{(1)}, \quad 0 < X < X_s, Z = 1. \tag{8.20}$$

https://doi.org/10.1017/jfm.2012.617 Published online by Cambridge University Press

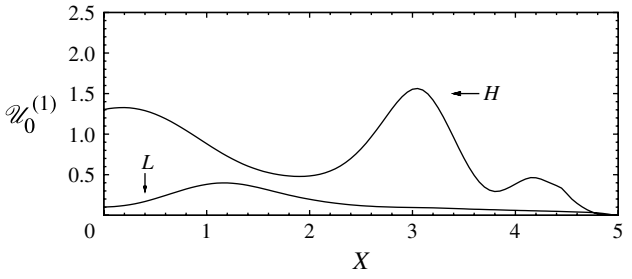


FIGURE 14. Cross-shore variation of the mean interface displacement for Hangzhou Bay mud (H) and Lianyun Harbor mud (L). Note that $10 \times \mathscr{U}_0^{(1)}$ is plotted for Lianyun Harbor. Inputs are the same as in figures 6 and 7.

Since $\mathscr{U}_0^{(1)} > 0$, the mud layer thickens as $X \to X_s$, in proportion to the shoreward displacement. As the seabed slope usually increases gradually from far offshore to the start of the beach, the vertical rise should gradually diminish in the offshore direction from $\mathscr{W}^{(1)}(0, 1)$.

9. Concluding remarks

We have developed an asymptotic theory for weakly nonlinear long waves over a thin mud layer. The fluid mud is modelled as a viscoelastic material with rheological properties depending on frequency. Based on the measured data of two field samples, the different effects of mud elasticity and viscosity are compared. In the course of propagation, nonlinearity causes harmonic generation in the leading-order waves, which induce oscillatory motion in mud. In turn energy is extracted from waves, leading to the attenuation of all harmonics. It is shown that over a sloping beach this interaction can be so effective as to damp out all waves before they reach the shoreline. By comparing two types of fluid mud with constitutive coefficients depending on frequency in different ways, it is found that quicker damping occurs in a mud with finer and more cohesive sediments. Higher harmonics due to nonlinearity are more effectively suppressed not only by greater viscosity but also by resonances as a consequence of elasticity. At the second order, nonlinearity in mud responds with a time-averaged shoreward displacement similar to the drift current in the oscillatory boundary layer of a viscous fluid. The displacement may in turn cause non-uniform thickening of the mud layer.

Many challenges remain for a more realistic modelling of mud/wave interactions. In the natural setting the vertical extent and density profile of the moving fluid mud depend on the wave climate and cannot be prescribed in advance of the solution. Transient fluidization, resuspension, deposition and consolidation should be accounted for in order to predict the continuous stratification across the lutocline on the top and the solidification at the bottom of the mud layer.

Acknowledgements

This research was funded by US Office of Naval Research as a part of the Multidisciplinary University Research Initiative (MURI) program under grant N00014-06-1-0718. For this collaboration Z.H.H. was supported by Earth Observatory of

https://doi.org/10.1017/jfm.2012.617 Published online by Cambridge University Press

Singapore. The authors thank the referee for commenting on the significance of resonance.

Appendix. Detailed expression of the drift displacement

The expression for the steady shear strain on the interface is

$$\left.\frac{\mathrm{d}\mathscr{U}_0^{(1)}}{\mathrm{d}Z}\right|_{Z=1} = \frac{1}{2}\frac{\epsilon\gamma^2}{G_0\kappa^2h^{3/2}}\sum_{m=1}|A_m|^2\,\mathrm{Re}\left(\mathscr{G}(\sigma_m)\sigma_{-m}^2\mu_{-m}\mathrm{sech}(\sigma_{-m})\right). \tag{A 1}$$

Recall that $\sigma_{-m}=\sigma_m^*$ and $\mu_{-m}=\mu_m^*$.

For later use, we write

$$\left.\frac{\mathrm{d}\mathscr{U}_0^{(1)}}{\mathrm{d}Z}\right|_{Z=1} = \frac{1}{2}\frac{\epsilon\gamma^2R}{G_0\kappa^2h^{3/2}}\sum_{m=1}\mathrm{Re}\left(\mathrm{i}m\,|A_m|^2\,\mathscr{P}_m(\sigma_m)\right) \tag{A 2}$$

with

$$\begin{aligned}\mathscr{P}_m(\sigma_m) &= \frac{\sigma_{-m}^2}{\mathrm{i}mR}\mathscr{G}(\sigma_m)\mu_{-m}\mathrm{sech}(\sigma_{-m}) = \frac{\mu_{-m}\mu_s}{\rho_M\omega d^2}\frac{\sigma_{-m}^2}{\mathrm{i}m}\mathscr{G}(\sigma_m)\mathrm{sech}(\sigma_{-m})\\ &= \frac{\mu'_{-m}}{\rho_M\omega d^2}\frac{\sigma_{-m}^2}{\mathrm{i}m}\mathscr{G}(\sigma_m)\mathrm{sech}(\sigma_{-m}).\end{aligned} \tag{A 3}$$

Use has been made of the definition of R in (4.9) and the normalization of the viscosity (5.24). The solution for $\mathscr{U}_0^{(1)}$ is

$$\mathscr{U}_0^{(1)} = \int_0^Z \mathrm{d}Z\int_1^{Z'}\mathrm{d}Z'F_m + \left.\frac{\mathrm{d}\mathscr{U}_0^{(1)}}{\mathrm{d}Z}\right|_{Z=0}. \tag{A 4}$$

Let us denote

$$\int H(\sigma_m,Z)\,\mathrm{d}Z = Q(\sigma_m,Z) \quad\text{and}\quad \int F(\sigma_m,Z')\,\mathrm{d}Z' = H(\sigma_m,Z). \tag{A 5}$$

The solution of $\mathscr{U}_0^{(1)}$ can be written as

$$\begin{aligned}\mathscr{U}_0^{(1)}(Z) = \frac{1}{2}\left(\frac{\rho_M\omega^2d^2}{G_0'}\right)\frac{\epsilon\gamma^2}{\kappa^2h^{3/2}}\mathrm{Re}\sum_{m=1}^{\infty}\mathrm{i}m\,|A_m|^2\\ \times\{Q(\sigma_m,Z)-Q(\sigma_m,0)+[\mathscr{P}_m-H(\sigma_m,1)]Z\}.\end{aligned} \tag{A 6}$$

https://doi.org/10.1017/jfm.2012.617 Published online by Cambridge University Press

The explicit expressions for $H(\sigma_m, Z)$ and $Q(\sigma_m, Z)$ are

$$\begin{aligned} H(\sigma_m, Z) = & \frac{\sigma_m}{\sigma_{-m}} \frac{(1/2 + 1/2 \tanh(\sigma_{-m}) \tanh(\sigma_m)) \sinh((\sigma_{-m} + \sigma_m) Z)}{\sigma_{-m} + \sigma_m} \\ & + \frac{\sigma_m}{\sigma_{-m}} \frac{(-1/2 + 1/2 \tanh(\sigma_{-m}) \tanh(\sigma_m)) \sinh((\sigma_{-m} - \sigma_m) Z)}{\sigma_{-m} - \sigma_m} \\ & + \frac{\sigma_m}{\sigma_{-m}} \frac{(-1/2 \tanh(\sigma_{-m}) - 1/2 \tanh(\sigma_m)) \cosh((\sigma_{-m} + \sigma_m) Z)}{\sigma_{-m} + \sigma_m} \\ & + \frac{\sigma_m}{\sigma_{-m}} \frac{(1/2 \tanh(\sigma_{-m}) - 1/2 \tanh(\sigma_m)) \cosh((\sigma_{-m} - \sigma_m) Z)}{\sigma_{-m} - \sigma_m} \\ & + \frac{\tanh(\sigma_m) (\sigma_m Z \sinh(\sigma_m Z) - \cosh(\sigma_m Z))}{\sigma_m} \\ & - \frac{\tanh(\sigma_{-m}) \tanh(\sigma_m) \sinh(\sigma_m Z)}{\sigma_{-m}} \\ & - \frac{\sigma_m Z \cosh(\sigma_m Z) - \sinh(\sigma_m Z)}{\sigma_m} + \frac{\tanh(\sigma_{-m}) \cosh(\sigma_m Z)}{\sigma_{-m}} \end{aligned} \tag{A 7}$$

and

$$\begin{aligned} Q(\sigma_m, Z) = & \frac{\sigma_m}{\sigma_{-m}} \frac{(1/2 + 1/2 \tanh(\sigma_{-m}) \tanh(\sigma_m)) \cosh((\sigma_{-m} + \sigma_m) Z)}{(\sigma_{-m} + \sigma_m)^2} \\ & + \frac{\sigma_m}{\sigma_{-m}} \frac{(-1/2 + 1/2 \tanh(\sigma_{-m}) \tanh(\sigma_m)) \cosh((\sigma_{-m} - \sigma_m) Z)}{(\sigma_{-m} - \sigma_m)^2} \\ & + \frac{\sigma_m}{\sigma_{-m}} \frac{(-1/2 \tanh(\sigma_{-m}) - 1/2 \tanh(\sigma_m)) \sinh((\sigma_{-m} + \sigma_m) Z)}{(\sigma_{-m} + \sigma_m)^2} \\ & + \frac{\sigma_m}{\sigma_{-m}} \frac{(1/2 \tanh(\sigma_{-m}) - 1/2 \tanh(\sigma_m)) \sinh((\sigma_{-m} - \sigma_m) Z)}{(\sigma_{-m} - \sigma_m)^2} \\ & + \tanh(\sigma_m) \left(\frac{\sigma_m Z \cosh(\sigma_m Z) - \sinh(\sigma_m Z)}{\sigma_m^2} - \frac{\sinh(\sigma_m Z)}{\sigma_m^2} \right) \\ & - \frac{\tanh(\sigma_m) \cosh(\sigma_m Z) \tanh(\sigma_{-m})}{\sigma_m \sigma_{-m}} \\ & - \left(\frac{\sigma_m Z \sinh(\sigma_m Z) - \cosh(\sigma_m Z)}{\sigma_m^2} - \frac{\cosh(\sigma_m Z)}{\sigma_m^2} \right) \\ & + \frac{\sinh(\sigma_m Z) \tanh(\sigma_{-m})}{\sigma_m \sigma_{-m}}. \end{aligned} \tag{A 8}$$

REFERENCES

BRYANT, P. 1976 Periodic waves in shallow water. *J. Fluid Mech.* **59**, 625–644.

COUSSOT, P. 1997 *Mud Flow Rheology and Dynamics*. Bakema.

DALRYMPLE, R. & LIU, P. L.-F. 1978 Waves over soft muds: a two-layer fluid model. *J. Phys. Oceanogr.* 1121–1131.

DALRYMPLE, R. A., NOURI, Y. & SABOURI-SHARGH, Z. 2008 Water waves propagating over mud. In *Proceedings of 31st International Conference of Coastal Engineering, vol. 1* (ed. J. M. Smith), vol. 1, pp. 314–323.

https://doi.org/10.1017/jfm.2012.617 Published online by Cambridge University Press

ELGAR, S. & RAUBENHEIMER, B. 2008 Wave dissipation by muddy seafloors. *Geophys. Res. Lett.* **35**, L07611.

GRATALOUP, G. & MEI, C. C. 2003 Localization of harmonics in nonlinear shallow water waves. *Phy. Rev.* E **68**, 02634.

HUANG, Z. H., HUHE, A. & ZHANG, Y. 1992 An experimental study of the properties of fluid mud in Xishu, Lianyungang (in Chinese). *Tech. Rep.* IMCAS STR-92019. Institute of Mechanics, Chinese Academy of Sciences.

HUANG, Z. H. & HUHE, A. 2009 A laboratory study of rheological properties of mudflows in Hangzhou Bay, China. *Intl J. Sedim. Res.* **24** (4), 410–424.

HUHE, A., HUANG, Z. H. & CHI, G. P. 1996 Experiments on the properties of cohesive sediments in Zhongshan Harbor, Jiangsu Province, Part II. In *Report in Chinese by Institute of Mechanics*. Chinese Academy of Sciences.

JIANG, F. & MEHTA, A. J. 1995 Mudbanks of the southwest coast of India IV: mud viscoelastic properties. *J. Coast. Res.* **11** (3), 918–926.

LIU, P. L.-F. & CHAN, I.-C. 2007*a* A note on the effects of thin visco-elastic mud layer on small amplitude water-wave propagation. *Coast. Engng* **54**, 233–247.

LIU, P. L.-F. & CHAN, I.-C. 2007*b* On long-wave propagation over a fluid-mud seabed. *J. Fluid Mech.* **579**, 467–480.

LIU, K. F. & MEI, C. 1989 Effects of water-induced friction on a muddy seabed modelled as a Bingham-plastic Fluid. *J. Coast. Res.* **5, 4**, 777–789.

LONGUET-HIGGINS, M. S. & STEWART, R. W. 1964 Radiation stresses in water waves, a physical discussion with applications. *Deep-Sea Res.* **11**, 529–562.

MAA, J. P-Y. & MEHTA, A. J. 1988 Soft mud properties: Voigt Model. *J. Waterways Port Coast. Ocean Engng* **114** (6), 765–770.

MACPHERSON, H. 1980 The attenuation of water waves over a non-rigid bed. *J. Fluid Mech.* **97**, 721–742.

MALVERN, L. E. 1969 *Introduction to the Mechanics of a Continuous Medium*. Prentice Hall.

MATHEW, J. & BABA, M. 1995 Mudbanks of the southwest coast of India, II: wave-mud interactions. *J. Coast. Res.* **11** (1), 179–187.

MEHTA, A. J. 1996 Interaction between fluid-mud and water waves. In *Environmental Hydraulics*, pp. 153–187. Kluwer, Chapter 5.

MEI, C. C. 1989 *The Applied Dynamics of Ocean Surface Waves*. World Scientific.

MEI, C. C. & LIU, K.-F. 1987 A Bingham-plastic model for a muddy seabed under long waves. *J. Geophys. Res. (Oceans)* **92** (C13), 14581–14594.

MEI, C. C., KROTOV, M., HUANG, Z. H. & HUHE, A. 2010 Short and long waves over a muddy seabed. *J. Fluid Mech.* **643**, 33–58.

MEI, C. C. & ÜNLÜATA, U. 1972 Harmonic generation in shallow water waves. In *Waves on Beaches* (ed. R. E. Meyer), pp. 181–202. Academic.

MILES, J. W. 1983 Solitary wave evolution over a gradual slope with turbulent friction. *J. Phys. Oceanogr.* **13**, 551–553.

NG, C. 2000 Water waves over a muddy bed: a two-layer Stokes' boundary layer model. *Coast. Engng* **40**, 221–242.

NG, C. & ZHANG, X. 2007 Mass Transport in Water waves over a thin layer of soft viscoelastic mud. *J. Fluid Mech.* **573**, 105–130.

PIEDRA-CUEVA, I. 1993 On the response of a muddy bottom to surface water waves. *J. Hydraul. Res.* **31**, 681–695.

ROGERS, S. R. & MEI, C. C. 1978 Nonlinear resonant excitation of a long and narrow bay. *J. Fluid Mech.* **88**, 161–180.

WAN, Z. H. 1994 *Hyperconcentrated Flows*. Balkema.

WELLS, J. T. 1978 Shallow water waves and fluid-mud dynamics. Coast of Surinam, South America. *Tech Rep.* 257. Coastal Studies Institute, Lousiana State University.

WELLS, J. T. & COLEMAN, J. M. 1981 Physical processes and fine-grained sediment dynamics, coast of Surinam South America. *J. Sedim. Petrol.* **51** (4), 1053–1068.

ZHANG, X. & NG, C. 2006 On the oscillatory and mean motions due to waves in a thin viscoelastic layer. *Wave Motion* **43**, 387–405.

https://doi.org/10.1017/jfm.2012.617 Published online by Cambridge University Press